

MotionGPT-2: A General-Purpose Motion-Language Model for Motion Generation and Understanding

Yuan Wang^{1,5,6†} Di Huang^{2‡} Yaqi Zhang³ Wanli Ouyang^{4,5}, *Senior Member, IEEE*
 Jile Jiao^{1,6} Xuetao Feng^{1,7} Yan Zhou⁸ Pengfei Wan⁸ Shixiang Tang^{4♣} Dan Xu⁹, *Member, IEEE*
¹Tsinghua University ²The University of Sydney ³University of Science and Technology of China
⁴The Chinese University of Hong Kong ⁵Shanghai Artificial Intelligence Laboratory ⁶Alibaba Group
⁷Deepleph ⁸Kuaishou Technology ⁹HKUST [‡]Equal Contribution [♣]Corresponding Author

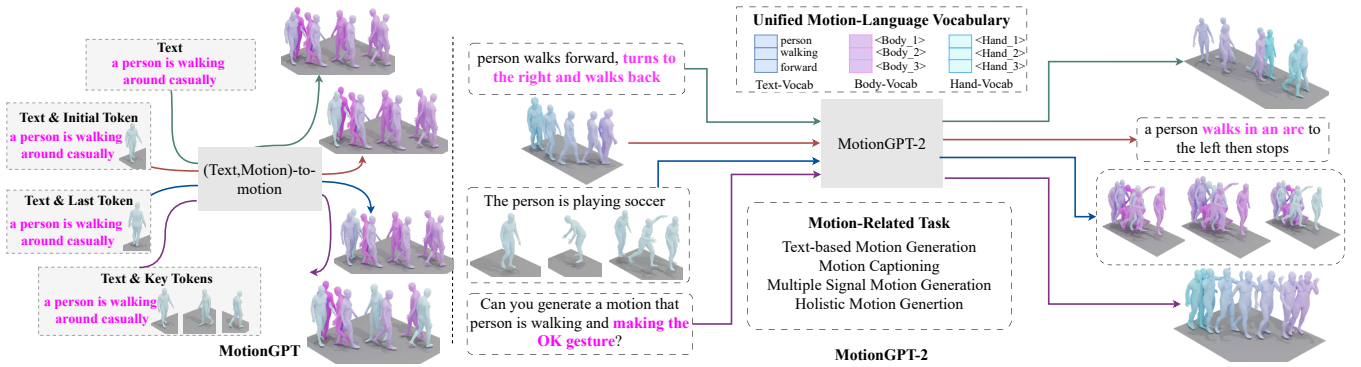


Fig. 1: This paper proposes a versatile motion-language framework via fine-tuned LLMs given different instructions, named MotionGPT-2. Compared with the previous MotionGPT [1], our MotionGPT-2 not only retains the unique capability of accommodating multiple control conditions, but also solve various motion-related tasks using a unified model.

Abstract—Generating lifelike human motions from descriptive texts has experienced remarkable research focus in the recent years, propelled by the emerging requirements of digital humans. Despite impressive advances, existing approaches are often constrained by limited control modalities, task specificity, and focus solely on body motion representations. In this paper, we present MotionGPT-2, a unified Large Motion-Language Model (LMLM) that addresses these limitations. MotionGPT-2 accommodates multiple motion-relevant tasks and supporting multimodal control conditions through pre-trained Large Language Models (LLMs). It quantizes multimodal inputs—such as text and single-frame poses—into discrete, LLM-interpretable tokens, seamlessly integrating them into the LLM’s vocabulary. These tokens are then organized into unified prompts, guiding the LLM to generate motion outputs through a pretraining-then-finetuning paradigm. We also show that the proposed MotionGPT-2 is highly adaptable to the challenging 3D holistic motion generation task, enabled by the innovative motion discretization framework, Part-Aware VQVAE, which ensures fine-grained representations of body and hand movements. Extensive experiments and visualizations validate the effectiveness of our method, demonstrating the adaptability of MotionGPT-2 across motion generation, motion captioning, and generalized motion completion tasks.

Index Terms—3D Human Motion Generation, Large Language Models, SMPL, Vector Quantized-Variational AutoEncoder

I. INTRODUCTION

HUMAN motion generation plays a pivotal role in various applications, including video gaming, robotic assistance, and virtual reality. Recent years have witnessed a rapid

development of Generative Artificial Intelligence (GenAI) [2]–[8], paving the way for novel methods to motion synthesis.

Despite the impressive performance achieved by existing motion generation methods [9]–[13], current methods suffer from three major limitations: (1) *Limited control conditions*. Existing approaches typically target only a single type of control condition, *i.e.*, either textual descriptions or multiple frame poses. This narrow scope constrains their practical applications in scenarios that require the generation of motion sequences conditioned on both text descriptions and multiple key-frame human poses, *e.g.*, social robotics and film animation. (2) *Task-specific frameworks without general world knowledge*. Existing models are often task-specific, such as diffusion-based and GPT-based frameworks [10], [14]–[16]. These methods lack the adaptability needed for multiple tasks (*e.g.*, captioning, in-betweening, prediction) and cannot fully leverage the world knowledge embedded in Large Language Models (LLMs). While recent work [17], [18] proposes unified frameworks, the full potential of LLMs in motion understanding and generation remains largely unexplored. (3) *Body-only motion representations*. Existing text-based motion generation solutions [10], [14], [16], [19], [20] primarily focus on generating body-only motions rather than holistic motions. However, their plausibility and expressiveness remain unsatisfactory in certain scenarios (*e.g.*, sports activities and playing musical instruments), as important details of human motion—*e.g.*, fine-grained hand gestures, are frequently overlooked.

To overcome these limitations, we propose MotionGPT-2, a unified Large Motion-Language Model (LMLM) capable of handling diverse control signals, performing various motion-relevant tasks, and generating holistic human motions. The key innovations of MotionGPT-2 include:

(1) **Formulating Multimodal Control Signals into a Unified Representation:** MotionGPT-2 designs a versatile framework and task-aware prompts for human motion synthesis. This framework, in particular, allows for the generation of human motions governed by multimodal control conditions, described by $M_{\text{out}}, T_{\text{out}} = f(T_{\text{in}}, \text{task}, M_{\text{in}})$. Here M_{in} and T_{in} refer to the input motions and texts, while M_{out} and T_{out} represent the resulting outputs. The variable task indicates the task-aware prompts that adapt the model to specific motion-related tasks. Compared to MotionGPT [1], MotionGPT-2 broadens the scope by incorporating additional motion-related tasks, *i.e.*, motion captioning, general motion completion.

(2) **Building a Task-Agnostic Framework with Strong Generalization:** Our conference version, MotionGPT [1], argued that this challenge can be naturally addressed with the assistance of LLMs. There are several compelling reasons. First, recent investigations indicate that LLMs have the ability to comprehend inputs from multiple modalities (*e.g.*, images [21]–[24] and videos [25]) through lightweight adapters [26]. Therefore, we expect that with suitable adapters, LLMs will be capable of understanding motion sequences. Secondly, LLMs have learned a broad range of motion patterns from their extensive text training, which allows them to offer diverse human motion contexts for generating motion. Consequently, our motion generator, adapted from LLMs, can produce motions with a wide range of rich patterns. Third, because LLMs generate tokens in a sequential manner, generating human motion with adaptable sequences is now easily achievable.

Our MotionGPT-2 improves MotionGPT [1] by using LLMs to jointly represent motion and language. We first embeds the human motions into discrete motion tokens via the Vector Quantized Variational-AutoEncoder (VQ-VAE). Then, we expand the LLM’s vocabulary with these motion tokens, creating an enriched motion-language vocabulary. By incorporating human motion and language into a unified vocabulary, the complex relationships between motion and language become transparent. Further, MotionGPT-2 integrates tokens from both language and motion prompts to generate instructions. We implement a multimodal pre-training combined with an instruction-tuning approach to train MotionGPT-2 efficiently, utilizing the established LoRA adaptation method. The motion instruction tuning framework we have developed allows for the integration of pose sequence information into the fine-tuned LLM, while capitalizing on the strong motion priors inherent in the origin LLM. With mere 1% parameters, the generalized MotionGPT-2 achieve competitive results in multiple motion-related tasks compared to those trained-from-scratch models with specialized frameworks.

(3) **Achieving Precise Discrete Representations of Holistic Human Motions:** To address this issue, we incorporate kinematic structure priors and design an innovative Part-Aware VQ-VAE for holistic motion tokenization. Compared to the vanilla motion VQ-VAE used in MotionGPT [1], the proposed

Part-Aware VQ-VAE utilizes two-level discrete codebooks and motion encoders to learn body-hand representations. The key insight of our Part-Aware VQ-VAE lies in its ability to learn informative and compact representations of fine-grained holistic motions. This two-level discretization framework captures subtle hand movements while maintaining global body dynamics. Finally, the hand and body motion tokens are integrated into the LLM’s vocabulary, enabling MotionGPT-2 to correctly interpret and generate holistic motion-related sequences in response to instructions.

We conduct extensive experiments on the HumanML3D [20], KIT-ML [27] dataset, demonstrating that MotionGPT-2 has strong adaptability and efficiency across multiple motion-related tasks by fine-tuning an LLM. With only 1% of additional parameters, MotionGPT-2 achieves competitive performance across tasks while significantly reducing training time—requiring only 10% of the time compared to other methods. We also observe that joint training under multiple control instructions surpasses training with singular control signals, highlighting the effectiveness of our unified motion-language fine-tuning paradigm. Experiments on the Motion-X [28] dataset verify that our proposed MotionGPT-2 is highly adaptable to the challenging 3D holistic motion generation task.

In summary, we extend our conference version [1] by **making several additional novel contributions:**

- We propose an enhanced version of the previous MotionGPT, MotionGPT-2. Compared to its predecessor, MotionGPT-2 serves as a unified Large Motion-Language Model to handle multiple motion-related tasks, enabling us to establish new state-of-the-art performance benchmarks.
- By creating an enriched motion-language vocabulary, we empower the pre-trained LLMs with the ability to unify the understanding and generation of body kinetics.
- We further extend the proposed MotionGPT-2 to tackle the challenging 3D whole-body motion generation task by introducing a whole-body motion discretization framework, **Part-Aware VQ-VAE**, which encodes body motions and hand gestures with two structured codebooks for fine-grained motion representations.

We conduct extensive experiments on the HumanML3D, KIT-ML, and Motion-X datasets to validate the superiority of our proposed LLM-based unified motion-language model across multiple motion-related tasks. We provide in-depth analysis and visualizations of MotionGPT-2, indicating that further advancements in LLM technology hold the potential to enhance its performance in the future.

II. RELATED WORK

A. LLMs and Multi-modal Large Language Models

Large Language Models (LLMs) [29]–[34] have experienced rapid development recently, *e.g.*, BERT [29], GPT [30], and Google T5 [35]. Notably, models like GPT-4 [33] show outstanding performance on various language tasks due to their extensive training datasets (GPT-4 utilizes 45 gigabytes) and numerous parameters. Traditionally, language models were crafted for specific tasks like translation or sentiment analysis,

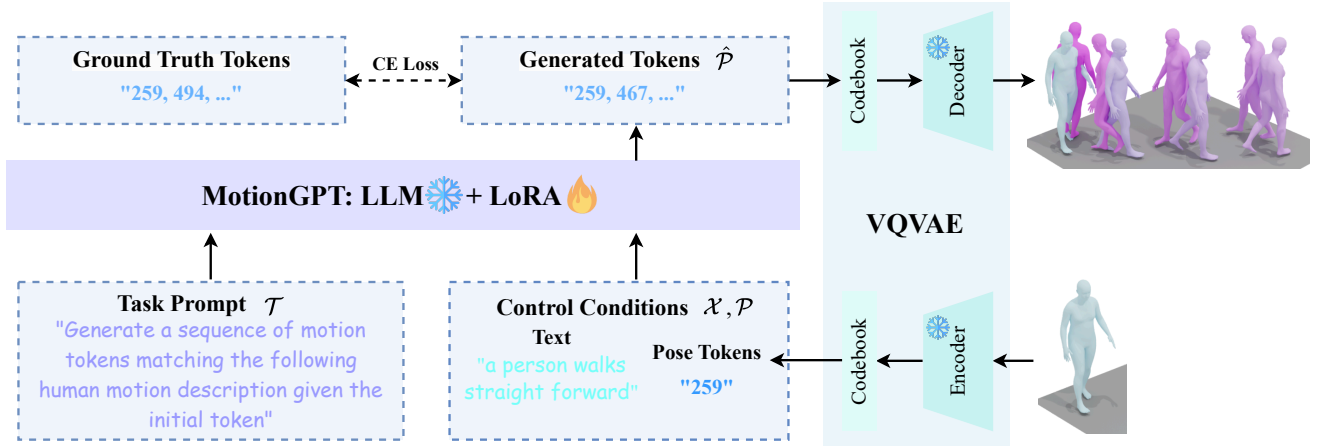


Fig. 2: The pipeline of MotionGPT, a Motion General-Purpose generator. Given text and poses as an input example, we organize task descriptions (Instruction) and multiple control conditions (Input) within a question template. MotionGPT fine-tunes an LLM to generate the corresponding motion answer, which can then be decoded into human motions using a VQ-VAE decoder.

but recent innovations, such as ChatGPT, have broadened their functional scope. Built on the GPT-4 framework, ChatGPT can engage in interactive dialogues, showcasing strong natural language understanding. This effectiveness opens new avenues for downstream applications achievable through the fine-tuning of these LLMs. Nevertheless, fine-tuning these extensive models poses significant challenges. To mitigate this issue, several efficient fine-tuning techniques have emerged, including prompt tuning [36]–[38], adapters [39]–[41], and LoRA [26]. Our study is inspired by recent developments in LLMs while tackling a different problem through the integration of a novel modality.

B. Human Motion Generation

Motion generation has a long-standing history in research [9]–[12], [42]–[46] and can be conditioned on various inputs, including motion descriptions, specific actions, and music. For instance, HP-GAN [47] and [48] adopt a sequence-to-sequence model to forecast future poses from earlier ones. Moreover, ACTOR [12] utilizes a transformer-based VAE for both unconditional generation and action-driven motion generation. TRAJEVAE [49] generates motion sequences that align with a given trajectory when provided with an initial pose. Recently, a significant focus has been placed on text-conditional motion generation, which involves creating human motion sequences based on textual prompts. Previous researches [14], [20], [42], [50], [51] focus on modeling a joint latent space for motion and text alignment. In TEMOS [9], a VAE model is proposed that creates a shared latent space for motion and text interactions. T2M-GPT [14] formulates the motion generation as the next index prediction task and leverage small language models to model the translation mapping between discrete motion indices and text. MotionCLIP [42] and TM2T [52] align the shared space of text and motion with the expressive CLIP [53] embedding space. MotionDiffuse [10] introduces a diffusion model into its framework for generating motion from textual descriptions, which leads to impressive outcomes. In a different approach, MDM [11] aims to boost the coherence between motion and textual inputs by implementing CLIP [53] as the

text encoder, thereby enhancing the model with more effective textual priors. However, it is challenging to model semantically complex relationships of human motions and texts, particularly in the absence of general world knowledge, *e.g.*, *how specific gestures convey intentions* and *how to interpret body language in different context*. Current efforts, such as MotionGPT [17], MotionLLM [54], M3-GPT [18] have initiated the development of a unified motion-language model aimed at generating plausible human motions alongside along with textual descriptions driven by prompt instructions. However, none of them leverage the general world knowledge of LLM simultaneously address diverse motion-related tasks and body-hand representations. Unlike prior approaches, MotionGPT-2 is distinguished as the first Large Motion-Language Model (LMLM) capable of multimodal control, handling diverse motion-related tasks, and providing a comprehensive representation of motion.

III. MOTION GENERAL-PURPOSE GENERATOR

Figure 3 depicts MotionGPT as a Motion General-Purpose generator that is driven by multi-modal inputs. To align with the LLM’s token-in-token-out nature, we first quantize the human motions into code representations via the well-established motion VQ-VAE [55] (Section III-A). These motion discrete codes, along with text control conditions and specially-crafted task-aware instructions, are organized into a unified question template (Section III-B). By adjusting the task-aware instructions, MotionGPT reveals its potential as a generic baseline framework for tasks involving motion generation.

A. 3D Human Motion Quantization

VQ-VAE proposed in [55] is designed to learn discrete representations with semantic-rich codebooks in an encoding-decoding fashion. To discretely represent human motions as semantic tokens, we introduce the motion VQVAE model, which consists of a motion encoder \mathcal{E} , a motion decoder \mathcal{D} , and a codebook $\mathcal{B}_m = \{b_1, b_2, \dots, b_N\}$, where N denotes the codebook size, as illustrated in Fig. 3. We denote a human

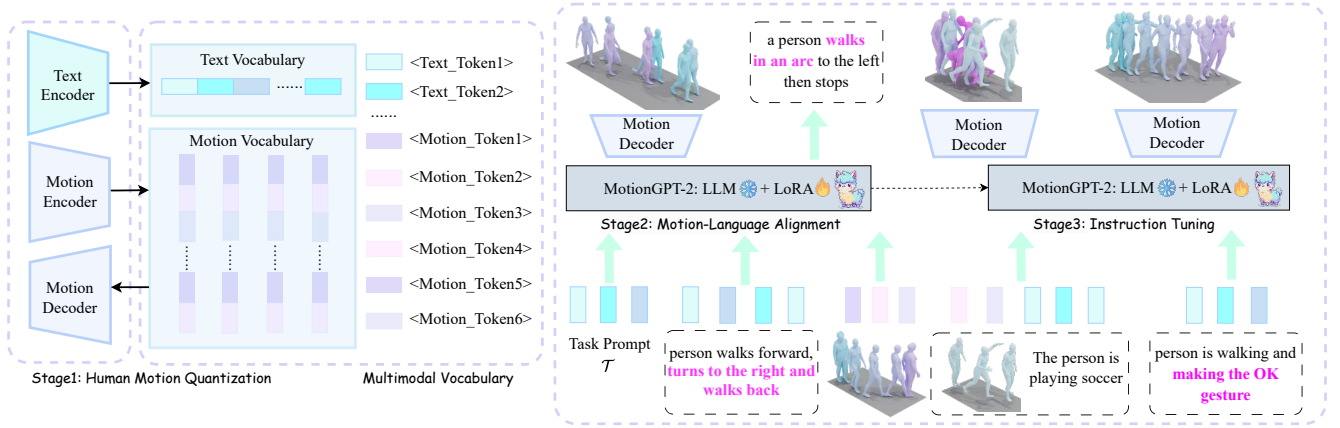


Fig. 3: The overview pipeline of our MotionGPT-2. MotionGPT-2 is composed of multi-modal tokenizers (Section III-A) and a versatile motion-language model (Section IV-B). With unified multimodal vocabulary and task-aware instructions (Section III-B), MotionGPT-2 enables to accept multiple control conditions (Section IV-C) and solve various motion-related tasks. MotionGPT-2 is learned by the *Motion-Language Alignment* stage and *Instruction Tuning* stage (Section IV-D).

motion as $\mathbf{m} = \{m_1, m_2, \dots, m_T\} \in \mathbb{R}^{T \times d}$, where T is the motion sequence length, and d is the dimension per frame.

To learn the codebook of human motions, the estimated motion embedding $\mathcal{E}(\mathbf{m})$ is transformed into a collection of codebook entries through quantization. Further, the quantized motion vector is obtained by searching the nearest corresponding embedding in a learnable codebook \mathcal{B}_m , which can be mathematically formulated as:

$$\mathbf{e} = \arg \min_{b_k \in \mathcal{B}} \|\mathcal{E}(\mathbf{m}) - b_k\|_2. \quad (1)$$

Based on the estimation latent representation \mathbf{e} , the motion decoder \mathcal{D} employs several 1-D deconvolutional layers to extract frame-wise motion features, decoding the sequential codes \mathbf{e} to the raw motion space as the motion $\hat{\mathbf{m}}$: $\hat{\mathbf{m}} = \mathcal{D}(\mathbf{e})$. The motion code p of the human pose \mathbf{m} can be calculated as the index of its nearest embedding in the codebook, *i.e.*,

$$p = \arg \min_k \|\mathcal{E}(\mathbf{m}) - b_k\|_2. \quad (2)$$

The standard motion VQ-VAE can be trained by the three tailored loss: 1) a reconstruction loss to minimize the distance between the decoded motion $\hat{\mathbf{m}}$ and the origin motion \mathbf{m} , 2) a codebook loss to encourage the b_k to be drawn closer to the encoded embedding $\mathcal{E}(\mathbf{m})$, aligning the discrete code representation with origin motion embeddings. 3) a commitment loss to guide the encoded embedding \mathbf{e} to remain close to the corresponding discrete code b_k , stabilizing the training process and reducing codebook oscillation. The total loss function $\mathcal{L}_{\text{VQVAE}}$ can be formulated as follows:

$$\mathcal{L}_{\text{VQVAE}} = \|\mathcal{D}(\mathcal{E}(\mathbf{m})) - \mathbf{m}\|^2 + \|\text{sg}[\mathcal{E}(\mathbf{m})] - \mathbf{e}\|_2^2 + \beta \|\mathcal{E}(\mathbf{m}) - \text{sg}[\mathbf{e}]\|_2^2. \quad (3)$$

Here, sg indicates the stop gradient operation and β is the hyper-parameter to control the weight of the commitment loss.

To enhance the quality of the generated motion, we incorporate *L1 smooth loss* and *velocity regularization loss* in the reconstruction loss. The codebook is optimized with Exponential Moving Average (EMA) operation and codebook reset techniques following [1], [14], [17].

B. Instruction Generation

In our previous conference version, we design instructions that integrate task prompts and control conditions to enable (text, motion)-motion generation tasks. Given the task prompts $\mathcal{T} = \{t_1, t_2, \dots, t_{n_t}\}$, the text control conditions $\mathcal{X} = \{x_1, x_2, \dots, x_{n_x}\}$ and the pose control conditions $\mathcal{P} = \{p_1, p_2, \dots, p_{n_p}\}$ where n_t , n_x and n_p are the number of codes in \mathcal{T} , \mathcal{X} and \mathcal{P} , the instruction template \mathcal{I} is formulated as:

% General control conditions format

Control Conditions: {The Text control condition \mathcal{X} $\langle x_1, x_2, \dots, x_{n_x} \rangle$ {The Pose control condition \mathcal{P} $\langle p_1, p_2, \dots, p_{n_p} \rangle$ }

% General instruction format

Instruction (\mathcal{I}): {The Task Prompt \mathcal{T} $\langle t_1, t_2, \dots, t_{n_t} \rangle$ {Control Conditions}}

Pose control conditions $\mathcal{P} = \{p_1, p_2, \dots, p_{n_p}\}$, representing pose codes produced by the previously mentioned motion VQ-VAE. The entire instruction \mathcal{I} is conceptualized as a series of specialized text inputs. By formulating diverse instruction prompts, the MotionGPT [1] tackles both traditional motion generation tasks and emerging challenges in motion synthesis.

Specifically, for text-based motion generation task, MotionGPT address it by instantiating following instruction \mathcal{I} :

Instruction (\mathcal{I}): {**Task Prompts:** “Generate a sequence of motion tokens matching the following human motion description.”} {**Control Conditions:** Text control condition \mathcal{X} }

By adjusting instructions, the proposed MotionGPT can be easily adapted to multiple control conditions, *e.g.* the textual description and an arbitrary number of human poses:

Instruction (\mathcal{I}): {**Task Prompts:** “Generate a sequence of motion tokens matching the following human motion description given the init/last/key pose tokens.”} {**Control Conditions:** Text control condition \mathcal{X} $\langle \text{Motion Token} \rangle$ }

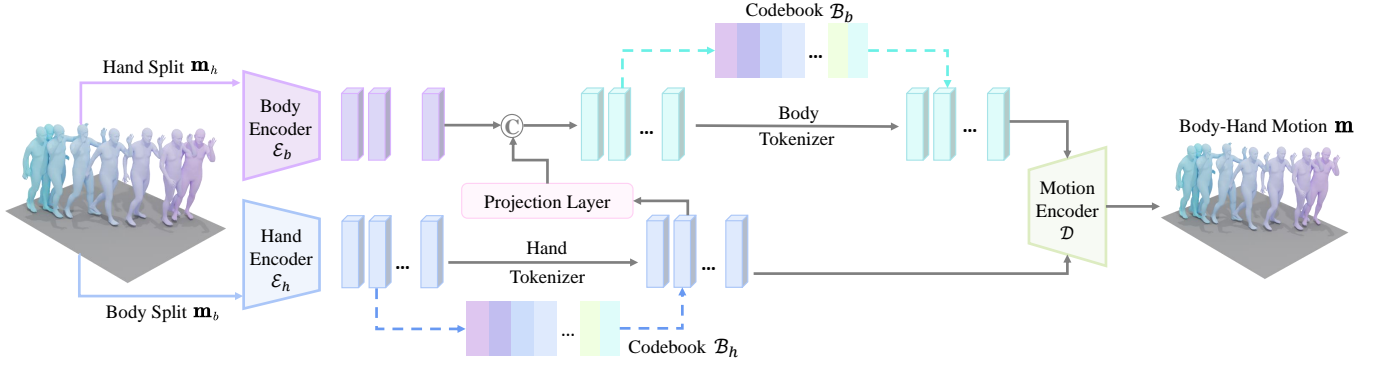


Fig. 4: The framework overview of our proposed Part-Aware VQVAE for body-hand motion tokenization. The Part-Aware VQVAE splits SMPL-X-based human representations into body-hand motions \mathbf{m}_b and \mathbf{m}_h . Then, it quantizes fine-grained body-hand motion into two discrete codebooks \mathcal{B}_b and \mathcal{B}_h with hierarchical body priors.

Pose control conditions $\mathcal{P} \langle \text{/Motion Token} \rangle \}$

For the motion generation task, the answer of LLM is represented as $\hat{\mathcal{P}} = \{\hat{p}_1, \hat{p}_2, \dots, \hat{p}_{n_{\hat{\mathcal{P}}}}\}$, comprising a sequence of generated motion codes. These codes can be decoded to human motion using Eq. 2.

C. Model Optimization

In the previous MotionGPT [1], we utilize a decoder-only LLM following [54], which effectively handle complex relationships and underlying patterns between text and motion. The token-in-token-out LLM maximizes the probability $p_{\theta}(x_t | x_{<t}, \mathcal{T}, c)$ of succeeding token in an autoregressive manner. Here, \mathcal{T} represents the Task Prompts, c is the control signal, $x_{1:T}$ denotes the target token sequence. Therefore, during the training process, the Cross Entropy loss is applied to ensure the correspondence between the estimated tokens and the real tokens, fine-tuning the LLM by LoRA [26], which is mathematically formalized as:

$$\mathcal{L}_{\text{LoRA}} = - \sum \log p_{\theta}(x_t | x_{<t}, \mathcal{T}, c). \quad (4)$$

IV. MOTIONGPT-2: A VERSATILE MODEL SUPPORTING HOLISTIC MOTION UNDERSTANDING AND GENERATION

Building upon the MotionGPT, MotionGPT-2 is to formulate a **multi-task unified** (motion generation, motion captioning, and generalized motion completion) framework to support **holistic motion representations** (fine-grained body and hand movements). The key designs are as follows: (1) *Part-Aware VQ-VAE for Body-hand Tokenization*. By designing an innovative Part-Aware VQVAE, our MotionGPT-2 achieves informative and compact representations of fine-grained holistic motions, making it adaptable to holistic motion generation tasks (Section IV-A). (2) *A Unified Motion-Language Vocabulary*. By expanding the text vocabulary of LLM, we develop a unified Large Motion-Language Model (LMLM) (Section IV-B) for the seamless integration of motion and language modalities. This vocabulary extension enables MotionGPT-2 to support a broader range of novel motion-related tasks by different instructions (Section IV-C). (3) *Three-Stage Training Strategy*. To enhance

the alignment between motions and texts, we develop a three-stage training pipeline (Section IV-D), including Motion Tokenization, Motion-Language Alignment, and Instruction Fine-tuning.

A. Part-Aware VQVAE for Holistic Motion Representations

Our previous MotionGPT is limited to the generation of body-only motions. Yet, advancing toward holistic motion generation is essential for achieving more realistic and lifelike animations. Holistic motions are considerably more complex than their body-only counterparts, necessitating the detailed and coordinated motion generation involving the body and hands features. In this section, our MotionGPT-2 emphasizes the representation of body-hand motions. With the above single motion vocabulary approach, the embedding of holistic human motion inevitably lead to ambiguities where similar actions are represented by the same motion token. To model distinct semantic granularity for body and hand, we design a Part-Aware VQVAE module, which utilizes the codebook \mathcal{B}_b and \mathcal{B}_h to learn discrete representations for body and hand, respectively.

Our proposed Part-Aware VQVAE is illustrated in Fig. 4. Specifically, we input the SMPL-X based body-hand representations $\mathbf{m}^B = \{m_1^B, m_2^B, \dots, m_T^B\} \in \mathbb{R}^{T \times d}$ and $\mathbf{m}^H = \{m_1^H, m_2^H, \dots, m_T^H\} \in \mathbb{R}^{T \times d}$ into two separate encoders. As shown in Fig. 4, the hand embedding \mathbf{e}_h is first quantized by the hand codebook \mathcal{B}_h and we then fuse the body and hand tokens via the concatenation operator before quantizing the body embedding \mathbf{e}_b using body codebook \mathcal{B}_b . The interaction between body and hand motions is tightly coupled and articulated, shaped by biomechanical and physical restrictions, particularly in the context of complex activities. Such a *fuse-before-quantize* method for body tokens effectively enhances the overall naturalness and coordination of holistic motion representations. Akin to the [56], the Body-hand Decoder is designed to take body tokens p^B and hand tokens p^H as input to accurately reconstruct corresponding motions.

B. A Unified Motion-Language Vocabulary

Most previous motion-related studies [1], [14], [19], [52], [57] have viewed textual descriptions and motions as separate

modalities. However, similar to sentences in natural language, a continuous motion \mathbf{m} is compressed into motion tokens, serving as a type of “body language”. Therefore, our MotionGPT-2 naturally uses LLMs to jointly model motion and language representations. It reflects how humans execute body motions, allowing for seamless transitions across motion-related modalities in real-life scenarios.

Specifically, to merge multi-modal discrete tokens with the pre-trained LLM, the original vocabulary \mathcal{B}_t is expanded to incorporate motion tokens \mathcal{B}_m . Further, we also insert several special tokens \mathcal{B}_s into the LLM’s vocabulary, *e.g.*, $\langle \text{motion} \rangle$ and $\langle / \text{motion} \rangle$, which signify the beginning and end of the motion. This extends the vocabulary into a unified text-motion set, $\mathcal{B} = \{\mathcal{B}_t, \mathcal{B}_m, \mathcal{B}_s\}$. The newly incorporated parameters are initialized randomly. Expanding the LLM’s vocabulary, a human motion is denoted as a token sequence that is LLM-understandable. Equipped with the vocabulary \mathcal{B} , we model the joint distribution of textual descriptions and human motions in a unified space. It allows us to formulate motion-related tasks in a general framework, leveraging the task-aware instructions.

C. Instruction Prompts in New Motion-Related Tasks

Our previous MotionGPT primarily focused on motion generation tasks. In contrast, our MotionGPT-2 enhances its capabilities by defining several core motion-related tasks, including motion captioning, motion prediction, and motion interpolation. For each task, we construct unique instruction prompts tailored to the specific task requirements. For instance, given a LLM \mathcal{F} , the instruction template \mathcal{I} for motion captioning and motion prediction task as well as the answer $\hat{\mathcal{P}}$ of the LLM $\hat{\mathcal{P}} = \mathcal{F}(\mathcal{I})$ are defined as:

Below is an instruction that describes a task, paired with an input that provides further context. Write a response that appropriately completes the request.

% Task Prompts: Motion Captioning Task Prompts

% Control Conditions: Code Sequences of Control Conditions (Motion Tokens)

Instruction \mathcal{I} : $\{\text{Task Prompts } \mathcal{T}\} \{\text{Control Conditions}\}$

Answer $\hat{\mathcal{P}}$: $\{\text{Sequences of Text Tokens}\}$

% Task Prompts: Motion Prediction Task Prompts

% Control Conditions: Code Sequences of Control Conditions (Initial Several Motion Tokens)

Instruction \mathcal{I} : $\{\text{Task Prompts } \mathcal{T}\} \{\text{Control Conditions}\}$

Answer $\hat{\mathcal{P}}$: $\{\text{Sequences of Human Motion Tokens}\}$

In the text-based holistic motion generation task, the instruction tuning phase proceeds after obtaining the discrete motion tokens p^B and p^H . During this stage, we formulate the instruction template \mathcal{I} and the answer \mathcal{P} of the LLM for motion generation. Inspired by MLLMs [21], [23], we unify the discrete body-hand tokens within a general prompt template.

Below is an instruction that describes a task, paired with an input that provides further context. Write a response that appropriately completes the request.

% Task Prompts: Motion Generation Task Prompts \mathcal{T}

% Control Conditions: Sequences of Control Conditions (Text Tokens)

Instruction \mathcal{I} : $\{\text{Task Prompts } \mathcal{T}\} \{\text{Control Conditions}\}$

Answer $\hat{\mathcal{P}}$: $\{\langle \text{Motion_Body_Token} \rangle \langle \text{Body_Token} \rangle \langle / \text{Motion_Body_Token} \rangle \langle \text{Motion_Hand_Token} \rangle \langle \text{Hand_Token} \rangle \langle / \text{Motion_Body_Token} \rangle\}$

D. Three-Stage Training Strategy

Our previous MotionGPT [1] is founded on a two-stage approach. Nevertheless, the absence of motion-language alignment hinders the model to interpret the complex relationships between motions and texts. Towards this issue, our MotionGPT-2 proposes a comprehensive three-stage training strategy:

Stage 1: Training of Motion Tokenizer. As depicted in Section III-A, we first learn the discrete motion representations to align with the LLM’s token-in-token-out nature. Guided by the objective outlined in Eq. 3, the quantization process allows human motions \mathbf{m} be expressed as a sequence of tokens, which seamlessly integrates with descriptive text. To maintain stability in LLM optimizing, we subsequently freeze the weights of the motion-aware VQVAE during further training stages.

Stage 2: Motion-Language Alignment. Inspired by current Multi-modal Large Language Models (MLLMs) [21], [23], to align the motion and language feature space of MotionGPT-2, the LLaMA [34] model is finetuned on a wide range of motion-related tasks. *To accurately interpret contextual ‘body language’ semantics while preserving the text generation capability of the LLM*, we finetune the LLM with LoRA using a mixture of language and motions data in both unsupervised and supervised manners. Similar to LLaVA [23], we learn the complex relationship of language and motions with the paired text-motion datasets. Further, we ensure the text generation capability through the LLM’s next-token prediction mechanism on text-only data. Compared with MotionGPT, with the additional motion-language alignment stage, MotionGPT-2 offers improved semantic consistency and fine-grained controls of human motions and textual descriptions.

Stage 3: Fine-tuning LLM by Motion Instructions. Instruction tuning [58] enables LLMs to handle various generation tasks by asking the LLM questions in different instructions. Hence, we devise a set of instructions that merge task descriptions with control signals and employ the efficient Low-Rank Adaptation (LoRA) [26] to fine-tune LLMs.

V. EXPERIMENTS

A. Experimental Setup

Datasets. We apply three publicly available datasets, HumanML3D [20], KIT-ML [27] and MotionX [28] for evaluation.

The HumanML3D dataset [20] stands as the largest available dataset focused solely on 3D body motion and associated textual descriptions. It comprises 14,616 motion clips paired with 44,970 meticulously annotated descriptions derived from a vocabulary of 5,371 unique words. These motion sequences are sourced from the AMASS [62] and HumanAct12 [45] motion capture collections, showcasing a diverse array of human activities, including everyday tasks, sports, acrobatics,

TABLE I: **Quantitative results of text-based motion generation on the HumanML3D dataset.** “Real” denotes the results computed with GT motions. “ \rightarrow ” indicates metrics that are better when closer to “Real” distribution. “MultiModal Dist.” denotes the Multi-Modality Distance. We conduct each evaluation 20 times, presenting the average metric and a 95% confidence interval, with the top scores marked in bold.

Model	Top 1	R-Precision \uparrow Top 2	Top 3	FID \downarrow	MultiModal Dist. \downarrow	Diversity \rightarrow	MultiModality \uparrow
Real	0.511 \pm .003	0.703 \pm .003	0.797 \pm .002	0.002 \pm .000	2.974 \pm .008	9.503 \pm .065	—
TM2T [52]	0.424 \pm .003	0.618 \pm .003	0.729 \pm .002	1.501 \pm .046	3.467 \pm .008	8.589 \pm .058	2.424 \pm .093
T2M [20]	0.457 \pm .002	0.639 \pm .003	0.740 \pm .003	1.067 \pm .002	3.340 \pm .008	9.188 \pm .002	2.090 \pm .083
MDM [59]	0.319 \pm .005	0.498 \pm .004	0.611 \pm .007	0.544 \pm .001	5.566 \pm .027	9.559 \pm .086	2.799 \pm .072
MotionDiffuse [10]	0.491 \pm .001	0.681 \pm .001	0.782 \pm .001	0.630 \pm .001	3.113 \pm .001	9.410 \pm .049	1.553 \pm .042
MLD [15]	0.481 \pm .003	0.673 \pm .003	0.772 \pm .002	0.473 \pm .013	3.169 \pm .010	9.724 \pm .082	2.413 \pm .079
T2M-GPT [14]	0.491 \pm .003	0.680 \pm .003	0.775 \pm .002	0.116 \pm .004	3.118 \pm .011	9.761 \pm .081	1.856 \pm .011
MoMask [16]	0.521 \pm .002	0.713 \pm .002	0.807 \pm .002	0.045 \pm .002	2.958 \pm .008	9.620 \pm .064	1.241 \pm .040
ReMoDiffuse [19]	0.510 \pm .005	0.698 \pm .006	0.795 \pm .004	0.103 \pm .004	2.974 \pm .016	9.018 \pm .075	1.795 \pm .043
AttT2M [60]	0.499 \pm .003	0.690 \pm .002	0.786 \pm .002	0.112 \pm .006	3.038 \pm .007	9.700 \pm .090	2.452 \pm .051
GraphMotion [61]	0.504 \pm .003	0.699 \pm .002	0.785 \pm .002	0.116 \pm .007	3.070 \pm .008	9.692 \pm .067	2.766 \pm .096
MotionGPT [1]	0.364 \pm .005	0.533 \pm .003	0.629 \pm .004	0.805 \pm .002	3.914 \pm .013	9.972 \pm .026	2.473 \pm .041
MotionGPT [17]	0.492 \pm .003	0.681 \pm .003	0.733 \pm .006	0.232 \pm .008	3.096 \pm .008	9.528 \pm .071	2.008 \pm .084
MotionLLM [54]	0.482 \pm .004	0.672 \pm .003	0.770 \pm .002	0.491 \pm .019	3.138 \pm .010	9.838 \pm .244	—
MotionGPT-2 (Ours)	0.496 \pm .002	0.691 \pm .003	0.782 \pm .004	0.191 \pm .004	3.080 \pm .013	9.860 \pm .026	2.137 \pm .022

and artistic expressions. Each motion clip is linked with 3-4 descriptive texts. For training, one sentence is randomly chosen as the match, while for testing, the first text description is consistently used to evaluate model performance. The motion clips are down-sampled to 20 FPS and vary in duration from 2 to 10 seconds. The dataset is divided into training, validation, and test subsets, allocated in an 80%, 5%, and 15% ratio, respectively, with no overlaps among them.

The KIT-ML [27] dataset is comprised of 3,911 motion sequences along with 6,278 textual descriptions. Each sequence is associated with one to four sentences, with the average description containing 9.5 words. This dataset merges selected elements from the KIT WholeBody Human Motion Database [63] and the CMU Graphics Lab Motion Capture Database [64], with an emphasis on locomotion motions. The motion sequences in KIT-ML have been down-sampled to a frame rate of 12.5 fps, ensuring a consistent and manageable speed for further analysis and experimentation.

The Motion-X [28] dataset is currently the largest whole-body expressive motion repository, comprising 95,642 high-fidelity 3D motion sequences based on the SMPL-X model [65], paired with corresponding pose descriptions and semantic labels for each sequence. The Motion-X dataset gathers 15K monocular videos from various online sources and public video dataset, capturing a wide range of scenarios such as daily actions, sports activities, and many domain-specific scenes, with 13.7M frame-level 3D whole-body pose annotations. In this paper, we standardize the Motion-X dataset by selecting 52 joints from the human body and hands.

Evaluation Metrics. Following [1], [14], [17], [20], [52], our evaluation metrics are summarized as the following parts:

(1) *Text-based Motion Generation Task.* To assess the quality of the generated motion, we utilize evaluation metrics that are aligned with those utilized in prior research. These metrics include the *Fréchet Inception Distance (FID)*, *Multi-modal*

Distance (MM Dist), *R-Precision* (calculating the Top-1/2/3 motion-to-text retrieval accuracy), the *Diversity*, and the *Multi-Modality* metric. Together, these metrics yield a comprehensive evaluation of the realism and diversity present in the generated motion. In accordance with the procedures outlined in [20], we calculate these metrics using a 95% confidence interval based on 20 independent trials.

(2) *Multiple Signal Controlled Motion Generation Task.* We propose new evaluation metrics for our motion generation framework: Reconstruction Loss (Recon) and Velocity Loss (Vel), both calculated using L2 loss to assess the alignment between the supplied pose conditions and the generated motion. When initial or final poses are specified, it is crucial that the corresponding generated poses appear correctly within the motion sequence. Therefore, we utilize *Recon* and *Vel* to assess the reconstruction of the initial or last poses and their temporal consistency with their surrounding poses. In cases where keyframe poses are provided but their positions of the corresponding generated poses within the sequence are unknown, we compute the Nearest Euclidean Distance to the corresponding ground truth poses and report the *Recon* and *Vel* to measure the key poses reconstruction and their temporal continuity with neighboring poses.

(3) *Motion-to-Text Task.* Besides R-Precision (Top-1/2/3) and multimodal distance, we also follow [17], [52] utilizing linguistic metrics from natural language studies, including BLEU [66], ROUGE [67], CIDEr [68], and BertScore [69], to quantitatively measure the performance of our MotionGPT-2 in the motion captioning task.

(4) *Motion Completion Task.* Beyond Diversity and FID metrics, we measure the accuracy of motion predictions using standard metrics such as Average Displacement Error (ADE) and Final Displacement Error (FDE), commonly utilized in prior works [17], [70], [71].

TABLE II: **Quantitative results of text-based motion generation on the KIT-ML dataset.** “Real” denotes the results computed with GT motions. “ \rightarrow ” indicates metrics that are better when closer to “Real” distribution.

Model	Top 1	R-Precision \uparrow Top 2	Top 3	FID \downarrow	MultiModal Dist. \downarrow	Diversity \rightarrow	MultiModality \uparrow
Real	0.424 \pm .005	0.649 \pm .006	0.779 \pm .006	0.031 \pm .004	2.788 \pm .012	11.080 \pm .097	—
TM2T [52]	0.280 \pm .005	0.463 \pm .006	0.587 \pm .005	3.599 \pm .153	4.591 \pm .026	9.473 \pm .117	3.292 \pm .081
T2M [20]	0.361 \pm .006	0.559 \pm .007	0.681 \pm .007	3.022 \pm .107	3.488 \pm .028	10.720 \pm .145	2.052 \pm .107
MDM [59]	0.164 \pm .004	0.291 \pm .004	0.396 \pm .004	0.497 \pm .021	9.191 \pm .022	10.850 \pm .109	1.907 \pm .214
MotionDiffuse [10]	0.417 \pm .004	0.621 \pm .004	0.739 \pm .004	1.954 \pm .062	2.958 \pm .005	11.100 \pm .143	0.730 \pm .013
MLD [15]	0.390 \pm .008	0.609 \pm .008	0.734 \pm .007	0.404 \pm .027	3.204 \pm .027	10.800 \pm .117	2.192 \pm .071
T2M-GPT [14]	0.416 \pm .006	0.627 \pm .006	0.745 \pm .006	0.514 \pm .029	3.007 \pm .023	10.920 \pm .108	1.570 \pm .039
MoMask [16]	0.433 \pm .007	0.656 \pm .005	0.781 \pm .005	0.204 \pm .011	2.779 \pm .022	10.711 \pm .087	1.131 \pm .043
ReMoDiffuse [19]	0.427 \pm .014	0.641 \pm .004	0.765 \pm .055	0.155 \pm .006	2.814 \pm .012	10.800 \pm .105	1.239 \pm .028
AttT2M [60]	0.413 \pm .006	0.632 \pm .006	0.751 \pm .006	0.870 \pm .039	3.039 \pm .021	10.960 \pm .123	2.281 \pm .047
GraphMotion [61]	0.429 \pm .007	0.648 \pm .006	0.769 \pm .006	0.313 \pm .013	3.076 \pm .022	11.120 \pm .135	3.627 \pm .113
MotionGPT [1]	0.340 \pm .002	0.570 \pm .003	0.660 \pm .004	0.868 \pm .032	3.721 \pm .018	9.972 \pm .026	2.296 \pm .022
MotionGPT [17]	0.366 \pm .005	0.558 \pm .004	0.680 \pm .005	0.510 \pm .016	3.527 \pm .021	10.350 \pm .084	2.328 \pm .117
MotionLLM [54]	0.409 \pm .006	0.624 \pm .007	0.750 \pm .005	0.781 \pm .026	2.982 \pm .022	11.407 \pm .103	—
MotionGPT-2 (Ours)	0.427 \pm .003	0.627 \pm .002	0.764 \pm .003	0.614 \pm .005	3.164 \pm .013	11.256 \pm .026	2.357 \pm .022

TABLE III: Assessment of motion generation on the HumanML3D [20] and KIT-ML [63] test subsets across diverse control conditions. With initial or key tokens, MotionGPT-2 demonstrate superior performance compared to the text-only version.

Methods	FID↓	MultiModal Dist.↓ HumanML3D (MotionGPT)	Diversity↑	FID↓	MultiModal Dist.↓ HumanML3D (MotionGPT-2)	Diversity↑
Text-Only	0.567	3.775	9.006	0.191	3.080	9.860
Text + Initial Pose	0.520	3.844	9.588	0.183	3.285	10.066
Text + Last Pose	0.591	3.718	9.251	0.358	3.673	9.582
Text + Random Pose	0.367	3.598	9.176	0.182	3.031	10.102
KIT-ML (MotionGPT)			KIT-ML (MotionGPT-2)			
Text-Only	0.597	3.394	10.540	0.614	3.164	11.256
Text + Initial Pose	0.664	3.445	10.390	0.756	3.362	11.053
Text + Last Pose	0.856	3.336	10.580	0.784	3.483	11.460
Text + Random Pose	0.671	3.411	10.760	0.807	3.173	11.447

B. Implementation Details

Motion Data Pre-processing. We follow the dataset pre-processing procedures outlined in [1], [14], [20]. The raw 3D motion coordinates are first aligned with a default human skeletal model. The Y-axis is then set perpendicular to the ground, allowing individuals to face the Z+ direction. These coordinates are then processed into motion features, including foot contact, global rotations and translations, local joint positions, velocities, and 6D rotations. The final dimensions are 263 for the HumanML3D dataset, 251 for the KIT-ML dataset, and 623 for the Motion-X dataset. For SMPL-based motion representations, the maximum motion length is set to 196, with minimums of 40 for HumanML3D and 24 for KIT-ML. In SMPL-X-based Motion-X dataset, the maximum motion length frames is 300, with a minimum of 40.

Training Details. In the following experiments, we adopt the decoder-only LLaMA 3.1-8B [34] model as the foundational LLM, keeping its parameters frozen while applying fine-tuning through the LoRA [26] method. The motion tokenizer is trained over 1,200 epochs, with an initial learning rate of 1×10^{-4} . We set the mini-batch size to 256 and use the AdamW optimizer [72], with a weight decay of 1×10^{-5} for

model optimization. Following previous studies [14], [17], we set the codebook $\mathcal{B}_m \in \mathbb{R}^{512 \times 512}$ for motion VQ-VAE and the codebook $\mathcal{B}_b \in \mathbb{R}^{512 \times 512}$ and $\mathcal{B}_h \in \mathbb{R}^{512 \times 512}$ for Part-Aware VQ-VAE. The motion encoder applies a temporal down-sampling rate of 4. Our MotionGPT-2 leverages a learning rate of 2×10^{-4} during the pre-training phase and 1×10^{-4} in the instruction tuning phase of the unified motion-language learning process. The mini-batch size is 32. The pre-trained LLM undergoes 100 epochs in the *Motion-Language Alignment* phase and 50 epochs during the *Instruction Tuning* phase. MotionGPT-2 and the re-implemented models are built using PyTorch, with all experiments on 4 NVIDIA 80G A100 GPUs.

C. Results on Human Motion Generation

Text-based Body-only Motion Generation. The quantitative results of motion quality are depicted in Table I, Table II, and Table III. Among these, Table I and Table II provide quantitative comparisons on the SMPL-based HumanML3D [20] dataset and the KIT-ML [63] dataset. The results presented reflect the performance of MotionGPT-2, which has been pre-trained across multiple motion-related tasks and subsequently fine-tuned for the specific text-based motion generation task. By

TABLE IV: Experiments of motion captioning task on the HumanML3D [20] benchmark. Results marked with * are from MotionGPT [17], and were computed using unprocessed ground truth texts for linguistic metrics.

Methods	R Precision \uparrow			MultiModal Dist. \downarrow	Length $_{\text{avg}}\uparrow$	Bleu1 \uparrow	Bleu4 \uparrow	Rouge \uparrow	Cider \uparrow	BertScore \uparrow
	Top1	Top2	Top3							
Real Desc	0.523	0.725	0.828	2.901	—	—	—	—	—	—
RAEs	0.100	0.188	0.261	6.337	—	33.3	10.2	37.5	22.1	10.7
Seq2Seq(Att)	0.436	0.611	0.706	3.447	—	51.8	17.9	46.4	58.4	29.1
SeqGAN	0.332	0.457	0.532	4.895	—	47.8	13.5	39.2	50.2	23.4
TM2T*	0.516	0.720	0.823	2.935	10.67	48.9	7.00	38.1	16.8	32.2
MotionGPT*	0.543	—	0.827	2.821	13.04	48.2	12.5	37.4	29.2	32.4
MotioGPT-2 (Ours)	0.558	0.738	0.838	2.767	15.27	48.7	13.8	37.6	29.8	32.6

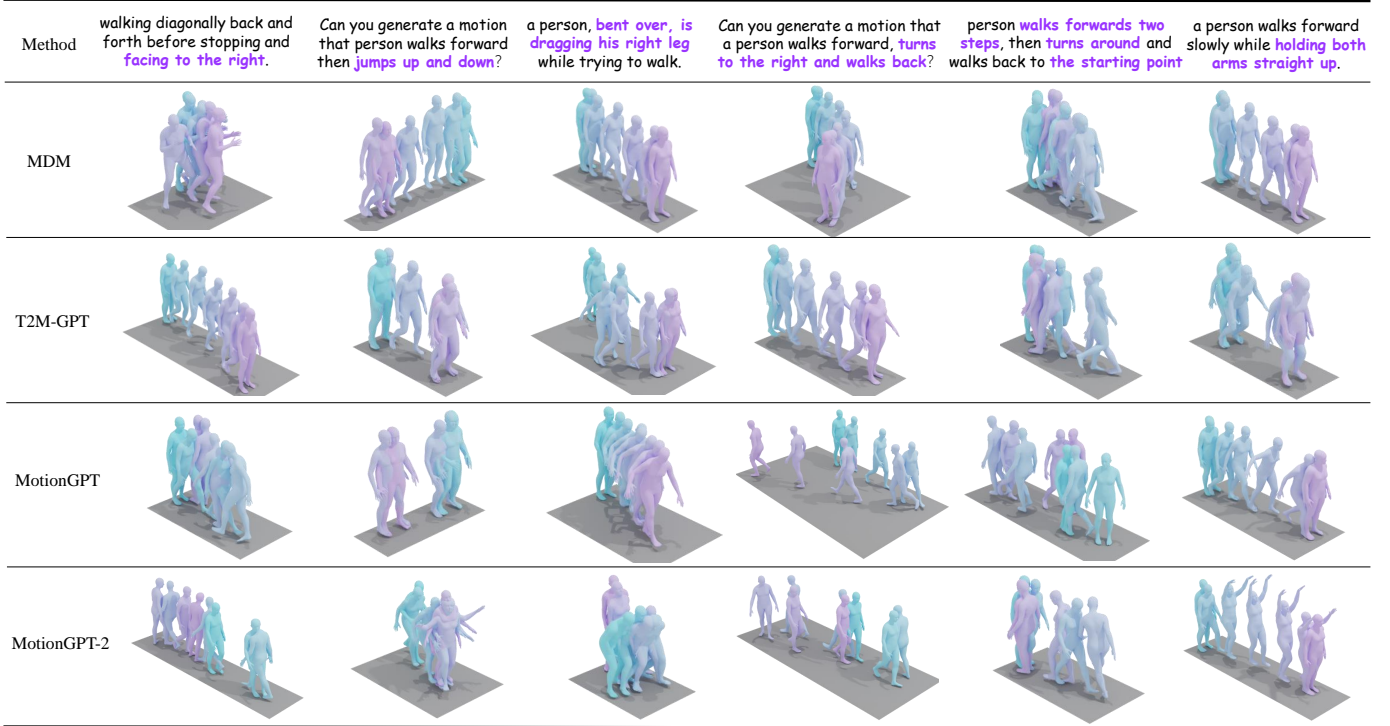


Fig. 5: Showcase of visualization results for the text-based motion generation task using the HumanML3D [20] dataset. We compare our MotionGPT-2 with the state-of-the-art method, *i.e.*, MDM [59], T2M-GPT [14], MotionGPT [1]. Compared with these methods, our MotionGPT-2 perform admirably to generate vivid human motions and preserve the semantic fidelity.

tuning mere 1% of LLM parameters, our general-purpose MotionGPT-2 exhibits a performance that is competitive with state-of-the-art approaches. Compared to our previous version, the MotionGPT-2 yields a significant **10.4%** improvement in R-Precision Top-3 and a **0.254** reduction in FID score on the HumanML3D dataset. Through the tailored *Motion-Language Alignment* stage, our MotionGPT-2 exhibits greater semantic consistency with the textual description, improving interpretation of body language semantics. Further, compared to other language model-based methods [17], [18], [54], our MotionGPT-2 fine-tunes the LLM and relate general world knowledge to 3D human motions, achieving superior generation capabilities beyond existing solutions.

As shown in Fig. 5 and Fig. 8, we further conduct visualization experiments on the text-based motion generation task to vividly illustrate the capabilities of our MotionGPT-2 model. In Fig. 5, we observe that the diffusion-based MDM [59]

method generates fewer semantic motions aligned with the provided descriptions. By utilizing discrete motion tokens, T2M-GPT [14] can better learn motion patterns and semantics which leads to more coherent and contextually rich motions. Our conference version MotionGPT [1], with fine-tuned LLMs, generalizes well to more diverse and complex text prompts. In contrast to MotionGPT, our MotionGPT-2 extends motion vocabulary to original LLMs for jointly modeling motion and language representations in a unified space. As demonstrated by the additional visualization results in Fig. 8, MotionGPT-2 shows high-fidelity motion and strong text prompt matching, which validates the effectiveness of our proposed method.

Multiple Signal Controlled Body-only Motion Generation.

Besides text inputs, MotionGPT-2 is capable of incorporating human poses as an additional control modality, with the resulting motion quality detailed in Table III. Introducing extra controls, such as initial, last, or key poses, does not

TABLE V: Ablations on the effects of LLM types and scales on text-based motion generation, evaluated on the HumanML3D [20] benchmark. In addition to full fine-tuning of the encoder-decoder T5-base model, LoRA-based fine-tuning [26] is used for optimizing other decoder-only LLMs.

Model	Trainable Parameters	R-Precision \uparrow			FID \downarrow	MultiModal Dist. \downarrow	Diversity \rightarrow	MultiModality \uparrow
		Top 1	Top 2	Top 3				
Real	—	0.511	0.703	0.797	0.002	2.974	9.503	—
T5-base (Pretrain)	Full-Finetune	0.314	0.457	0.554	0.493	4.662	9.634	1.793
T5-base (Finetune)	Full-Finetune	0.417	0.581	0.668	0.148	3.989	9.961	1.985
Gemma-2b-It (Pretrain)	34M	0.385	0.546	0.643	0.207	4.559	9.733	2.351
Gemma-2b-It (Finetune)	34M	0.436	0.600	0.697	0.228	3.589	10.081	2.269
Gemma-7b-It (Pretrain)	101M	0.404	0.575	0.673	0.219	3.768	9.964	2.364
Gemma-7b-It (Finetune)	101M	0.446	0.622	0.715	0.177	3.545	9.652	2.198
LLaMA3-8B (Pretrain)	89M	0.438	0.619	0.717	0.314	3.514	10.010	2.252
LLaMA3-8B (Finetune)	89M	0.482	0.668	0.760	0.282	3.288	10.212	2.261
LLaMA3.1-8B (Pretrain)	89M	0.456	0.630	0.732	0.291	3.417	9.884	2.145
LLaMA3.1-8B (Finetune)	89M	0.496	0.691	0.782	0.191	3.080	9.860	2.137

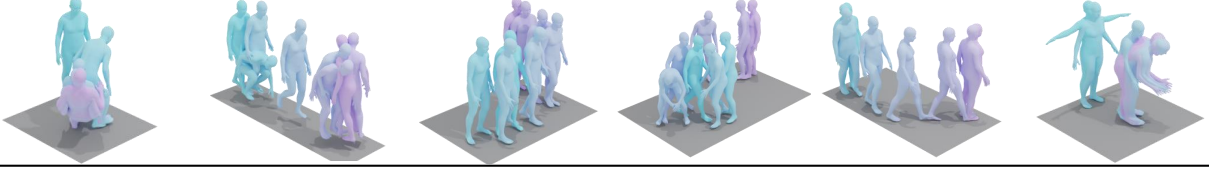
Input Motions						
						
Real	a person turns around, sits down , and leans back .	a person walks forward, picks something up off of the floor, then puts it on a low shelf or object.	the toon is walking in a zig zag motion, shuffling a bit at the end of the "plane"	a person throws something , then catches something, then throws it	person walks forward and curves to the left .	person starts out with both arms extended, takes two steps forwards, wipes something vigorously using right hand
MotionGPT	a person slowly turns around and then lies down	a person is walking forward, grabs something, turns around, and sit the object down.	this person walks in a zig zag motion from back to front	a person throws something and then catches something.	person is standing still, slightly shifting their weight to the left.	a person takes two steps forward and then uses their hand to clean something.
Ours	a person turns and sits in a chair , then gets back up .	a person walks forward. they stop and bend down to pick something up , then continue walking.	a man strolls slowly , and staggers to the left in a zig zag pattern	person looks like he is throwing a baseball then catches one and throws it again	a person walks in an arc to the left then stops.	a person walks two steps forward and makes a scrubbing motion with his right hand .

Fig. 6: Comparison of the state-of-the-art method on the motion captioning task. The results demonstrate that our MotionGPT-2 outperforms the MotionGPT on the HumanML3D [20], generating more conceptually and semantically rich motion descriptions. Specific words are marked to highlight the semantic similarity of the generated captions and the real one. Best viewed in color.

degrade motion quality. In fact, MotionGPT-2 shows superior performance when initial or key tokens are provided, achieving FID scores of **0.183** or **0.182**, an improvement over the text-only model's 0.191 on the HumanML3D benchmark, demonstrating its flexibility in handling diverse control modalities. In fact, MotionGPT-2 shows superior performance when initial or key tokens are provided, achieving FID scores of **0.183** or **0.182**, an improvement over the text-only model's 0.191 on the HumanML3D benchmark. In spite of this, MotionGPT-2's performance is still notable, reinforcing its proficiency in generating high-quality and diverse motions across a range of control conditions. As demonstrated in Fig. 9, the motions produced by our model align closely with the specified poses and consistently follow the textual descriptions.

Holistic Motion Generation. In this part, we focus on the holistic motion generation task. As shown in Table XI, we evaluate various LLMs on the SMPL-X-based Motion-X [28] dataset. Our tailored PA-VQVAE consistently outperforms the original VQVAE across multiple scales and types of LLMs, demonstrating the effectiveness of our innovative motion discretization framework. For instance, compared to

its VQVAE counterpart, Part-Aware VQVAE (LLaMA 3.1-8B) achieves an improvement in Top-1 R-Precision from 0.332 to 0.349, and a decrease in FID from 0.666 to 0.619. The superior performance of Part-Aware VQVAE over the original VQVAE can be attributed to its more fine-grained discretization representation and hierarchical modeling capability for human motion. Moreover, utilizing distinct motion vocabularies for body and hand reduces the ambiguity, where similar actions could be represented by the same token. As shown in Fig. 7, our MotionGPT-2 is capable of generating vivid motions that accurately correspond to the given text descriptions, particularly highlighting subtle hand movements such as *playing the piano*, *flying a kite*, and *stapling papers*.

D. Results on Motion Captioning

Compared to the text-to-motion task, the motion-to-text task involves generating a textual description from a given human motion sequence. As in [17], we rely on ground truth descriptions for more accurate assessment. Table IV presents the results of quantitative evaluation for motion-to-text translation on the HumanML3D dataset. The comparisons in Table IV

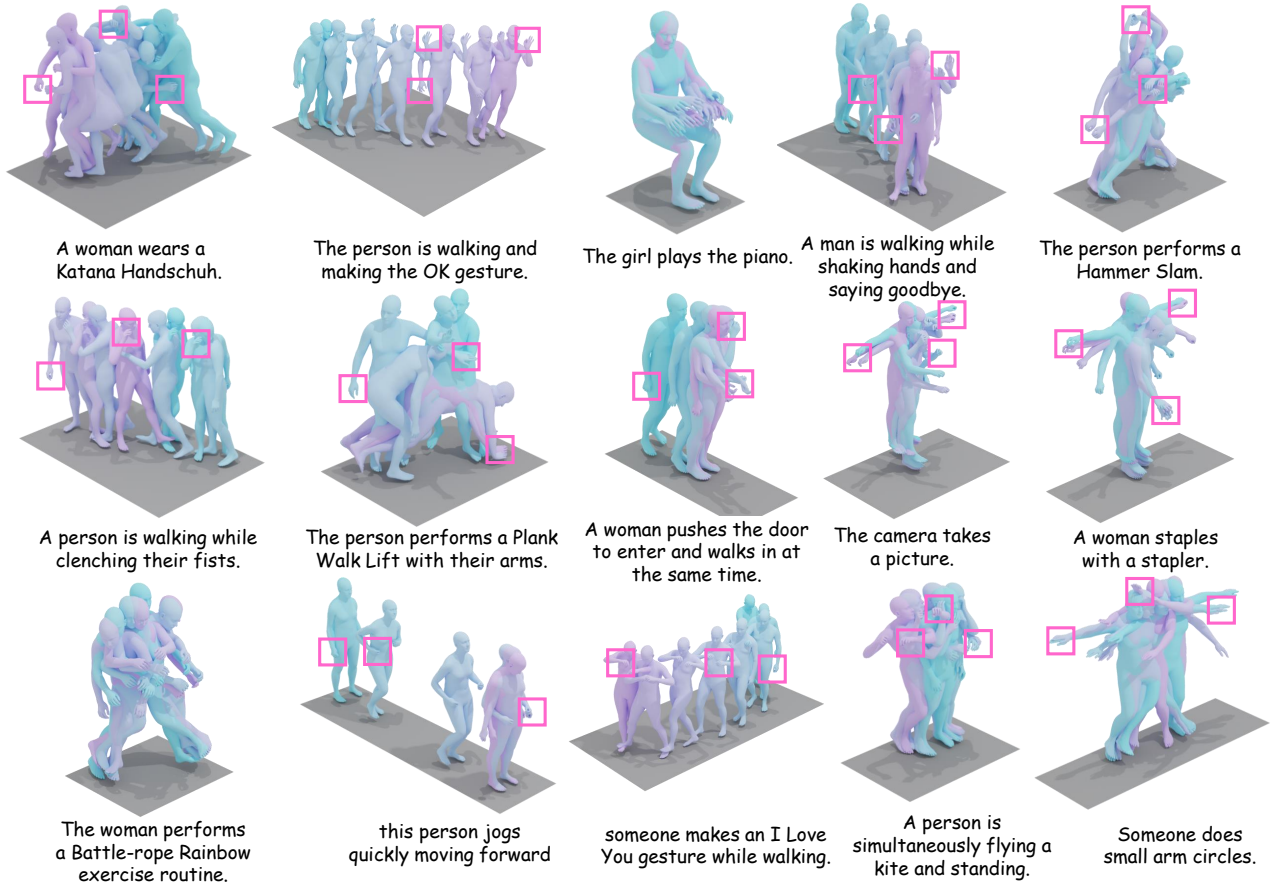


Fig. 7: Qualitative results of our proposed method on the Motion-X [28] dataset. Utilizing the world knowledge of LLMs, our MotionGPT-2 demonstrates the capability to generate realistic body motions while effectively capturing lifelike hand interactions, e.g., *making the OK gesture*, *plays the piano*, *saying goodbye*.

TABLE VI: Ablations on the effects of LLM types and scales on text-based motion generation, evaluated on the KIT-ML [63] benchmark. Along with full fine-tuning of the T5-base model, LoRA-based fine-tuning [26] is used for optimizing other LLMs.

Model	Trainable Parameters	R-Precision \uparrow			FID \downarrow	MultiModal Dist. \downarrow	Diversity \rightarrow	MultiModality \uparrow
		Top 1	Top 2	Top 3				
Real	—	0.424	0.649	0.779	0.031	2.788	11.080	—
T5-base	Full-Finetune	0.358	0.575	0.683	0.983	3.508	10.877	2.328
Gemma 2B-It	34M	0.364	0.581	0.699	1.063	3.424	10.603	2.150
Gemma 7B-It	101M	0.385	0.596	0.730	0.956	3.333	10.951	2.416
LLaMA 3-8B	89M	0.394	0.605	0.734	0.816	3.214	11.055	2.167
LLaMA 3.1-8B	89M	0.427	0.627	0.764	0.614	3.164	11.256	2.357

shows that our proposed MotionGPT-2 outperforms recent works in generating text descriptions for the given motions. The generated language descriptions deliver substantial improvements in both linguistic quality (BLEU [66] and BertScore [69]) and the precision of motion retrieval (R-Precision). By fine-tuning LLMs, our MotionGPT-2 emerges as a specialized tool endowed with extensive world knowledge, thereby enhancing its capacity to interpret human motion.

In Fig. 6, we provide further examples of translating motion to text using the HumanML3D dataset. All methods are evaluated under the same training and inference conditions on HumanML3D. Compared to MotionGPT [17], our MotionGPT-2, which leverages LLM-interpretable motion tokens, is capable

of generating more conceptual and semantically rich motion descriptions. For instance, it can produce descriptions such as “*walk in an arc shape*”, “*throwing a baseball*”, “*sits in a chair*”, offering a clearer and more intuitive understanding of the given motion motions.

E. Results on Generalized Motion Completion

Following [17], we classify both motion prediction and in-betweening together as generalized motion completion in Table X. For the motion prediction task [70], [71], [73], only the first 20% of the sequence is used as the conditioning input, while approximately 50% of the motion is intentionally masked at random to assist in the completion process. Similar

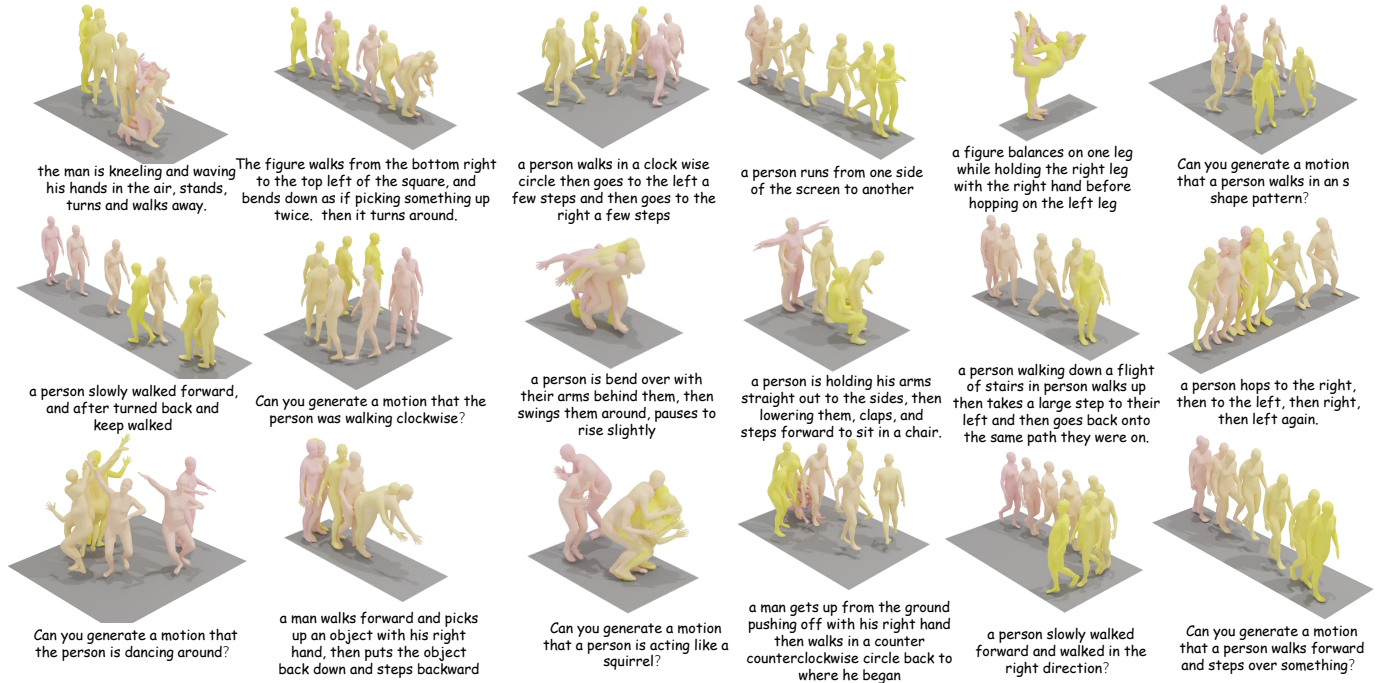


Fig. 8: More text-based human motion samples generated by our proposed MotionGPT-2 (with LLaMA 3.1-8B) using texts from the HumanML3D test set. Our method effectively generates a diverse range of dynamic and imaginative motions, *e.g.*, “acting like a squirrel”, “walking in an S-shaped pattern”, and “dancing around”.

Initial token	Recon MotionGPT	Vel MotionGPT	Recon MotionGPT-2	Vel MotionGPT-2
Text-only	24.70	1.095	19.19	0.846
Text + Initial poses	13.78	0.549	7.59	0.328
Last token	MotionGPT		MotionGPT-2	
Text-only	19.70	1.172	11.77	0.735
Text + Last poses	6.831	0.397	4.376	0.291
Key tokens	MotionGPT		MotionGPT-2	
Text-only	8.035	3.813	6.591	1.932
Text + Random poses	5.383	2.423	4.139	1.055

TABLE VII: Evaluation of the consistency with pose control conditions on the HumanML3D [20] test sub-set using the pre-trained LLaMA 3.1-8B model. In contrast to text-only generation, the incorporation of pose conditions enhances the consistency of key-frame poses during the generation process.

to text-based motion generation, as shown in Table X, we also fine-tune the proposed MotionGPT-2 specifically for this specific task and utilize FID, ADE, and FDE as metrics. The unified motion-language framework of the MotionGPT-2 leverages contextual information of fine-tuned LLM to understand in-depth motion dynamics. Compared to [17], [59], our MotionGPT-2 demonstrates a remarkable capability to generate contextually appropriate motion completions.

F. Ablation Study

Capability of Pre-trained LLM. As demonstrated in Table V and Table VI, we delve into how different scales and types of LLMs affect the performance of text-based human motion

generation tasks on the HumanML3D [20] and KIT-ML [63] datasets. We observe that: (1) Larger LLMs (*e.g.*, LLaMA 3.1-8B and LLaMA 3-8B) offer distinct advantages over smaller counterparts, achieving significant improvements in fidelity (FID) and multimodal alignment (*i.e.*, R Precision, MultiModal Dist.). To explain, the improved context understanding of LLMs ensures that the output motion aligns closely with intended actions. Further, LLMs with comprehensive world knowledge can synthesize physically plausible motions even when faced with linguistic ambiguity. (2) LLMs fine-tuned by unified instructions demonstrate clear advantage in maintaining semantic consistency and producing motions that are better aligned with textual descriptions. For instance, the fine-tuned Gemma-7B-It outperforms its pre-trained counterpart, achieving a 10% improvement in R-Precision Top-3 (from 0.673 to 0.715) and a 19% reduction in FID (from 0.219 to 0.177). (3) Compared to T5-base used in [17], [18], which requires full fine-tuning, fine-tuning the decoder-only LLaMA 3.1-8B yields a higher R-Precision Top-3 (0.782) and a lower FID (0.191). This indicates that larger models with more parameters possess a greater capacity to capture complex relationships between text and motion, enhancing both precision and diversity.

Consistency with pose control conditions. We assess the benefits of pose control by comparing the consistency between the controlled poses and the generated motions on the HumanML3D test sub-set. Concerning each specific task (initial/last/key), motions are generated both with and without pose controls, utilizing the (text+pose)-to-motion and text-to-motion methods, respectively. The results, displayed in Tab. VII indicate that key-frame consistency is higher with pose controls than in text-only generation counterpart, proving

TABLE VIII: Comparisons between separate training for each task and joint training for multiple tasks on HumanML3D [20] test set using the LLaMA 3-8B model. We use orange and green markings to represent decrements and improvements in the metric, respectively. Joint training can achieve better performance for all tasks.

Task	Training Strategy	FID ↓	MultiModal Dist. ↓	Top-1	R-Precision ↑ Top-2	Top-3	Diversity ↑
Text	Separate	0.523	3.627	0.358	0.514	0.604	9.108
+ Initial token		0.483	3.489	0.378	0.549	0.647	9.614
+ Last token		0.974	4.208	0.339	0.501	0.598	9.598
+ Key tokens		0.428	3.276	0.424	0.617	0.697	9.929
Text	Joint	0.482(-0.041)	3.295(-0.332)	0.419(+0.061)	0.597(+0.083)	0.683(+0.079)	9.422(+0.314)
+ Initial token		0.454(-0.029)	3.173(-0.316)	0.434(+0.056)	0.613(+0.064)	0.710(+0.063)	9.573(-0.041)
+ Last token		0.507(-0.467)	3.860(-0.348)	0.427(+0.088)	0.608(+0.107)	0.723(+0.125)	9.688(+0.090)
+ Key tokens		0.406(-0.022)	3.459(-0.183)	0.445(+0.021)	0.616(-0.001)	0.722(+0.025)	9.987(+0.058)

TABLE IX: Evaluation of text-based human motion generation using the LLaMA 3-8B model with various prompts on the HumanML3D [20] test subset.

Prompts	FID ↓	MultiModal Dist. ↓	R-Precision ↑			Diversity ↑
			Top-1	Top-2	Top-3	
V_1	4.196	5.275	0.357	0.542	0.658	8.110
V_2	2.692	4.573	0.418	0.603	0.719	8.534
V_0 (Ours)	0.191	3.080	0.482	0.669	0.760	9.860

the effectiveness of (text+pose)-to-motion with pose control. Such results highlight the critical role that pose controls play in coherent and contextually appropriate human motion synthesis.

Comparison with Separate Training. We carry out task-specific training on the HumanML3D dataset [20] to test the effectiveness of the proposed MotionGPT-2 model in motion generation. This experimental setup is implemented to determine whether a multi-task learning framework can enhance the performance of each distinct control condition independently. The comparison results are presented in Table VIII. Our findings indicate that joint training across all tasks significantly improves performance metrics across the board. Notably, this enhancement is particularly pronounced when utilizing text and the last pose token as input conditions. These results illustrate the value of our multi-modal signals controlled motion generation. MotionGPT-2’s ability to generate motions under a specific input condition is strengthened by drawing knowledge from other conditions.

Hyper-parameters of LoRA. The LoRA [26] method provides the source for all trainable parameters during training, with two key hyper-parameters: r and α . The rank of LoRA parameters is represented by r , with lower values corresponding to fewer parameters. α adjusts the scale of the dense layer’s outputs in LoRA. According to Table XII, we find that increasing r , while holding α constant, improves our model’s performance on nearly all metrics. Keeping the scale factor $\frac{\alpha}{r}$ equivalent to the learning rate demonstrates that increasing r yield better results. Moreover, we observe that adjusting α with a fixed r gives optimal performance when $\alpha = 16$.

Evaluation of Prompt Design. LLM are highly responsive to the way prompts are structured, which underscores the importance of meticulously crafting prompts to enhance the effectiveness of the model. This section explores the influence of using two alternative prompt and evaluates their individual

performances. We refer to the prompt utilized in our model as V_0 , while also presenting two supplementary prompts, V_1 and V_2 as follows:

% Prompts V_1

Human motion can be represented by token indices by VQ-VAE. Below is an instruction that describes human motion generation condition types, paired with an input that provides specific conditions. Write a sequence of tokens matching with given conditions.

Instruction (\mathcal{I}) : {**Task Prompts:** "Motion description(and the init/last/key pose tokens)."} {**Control Conditions:** Text control condition \mathcal{X} (< Motion Token > Pose control conditions \mathcal{P} < Motion Token >) }

% Prompts V_2

Below is an instruction that describes a task, paired with an input that provides further context. Write a response that appropriately completes the request.

Instruction (\mathcal{I}) : {**Task Prompts:** "Generate the token sequence of the motion description (under the premise of given init/last/key pose tokens)."} {**Control Conditions:** Text control condition \mathcal{X} (< Motion Token > Pose control conditions \mathcal{P} < Motion Token >) }

Regarding the prompts V_1 , we embed specific details regarding human motion generation into the overall descriptions, simplifying the task prompts to concentrate on the types of conditions alone. In contrast, we revise the task prompts for the V_2 , we modified the expression of the task prompts. Table IX presents the comparative results, illustrating the effectiveness and importance of the proposed prompt designs.

VI. CONCLUSION AND LIMITATIONS

A. Conclusion

In this paper, we introduce the MotionGPT-2, a versatile Large Motion-Language Model (LMLM), which can generate and comprehend human motions with general world knowledge of LLMs. Notably, MotionGPT-2 unifies motion-related tasks with multi-modal control signals (e.g., text and single-frame poses) as input by discretizing pose conditions and creating a unified set of instructions from combined textual and pose

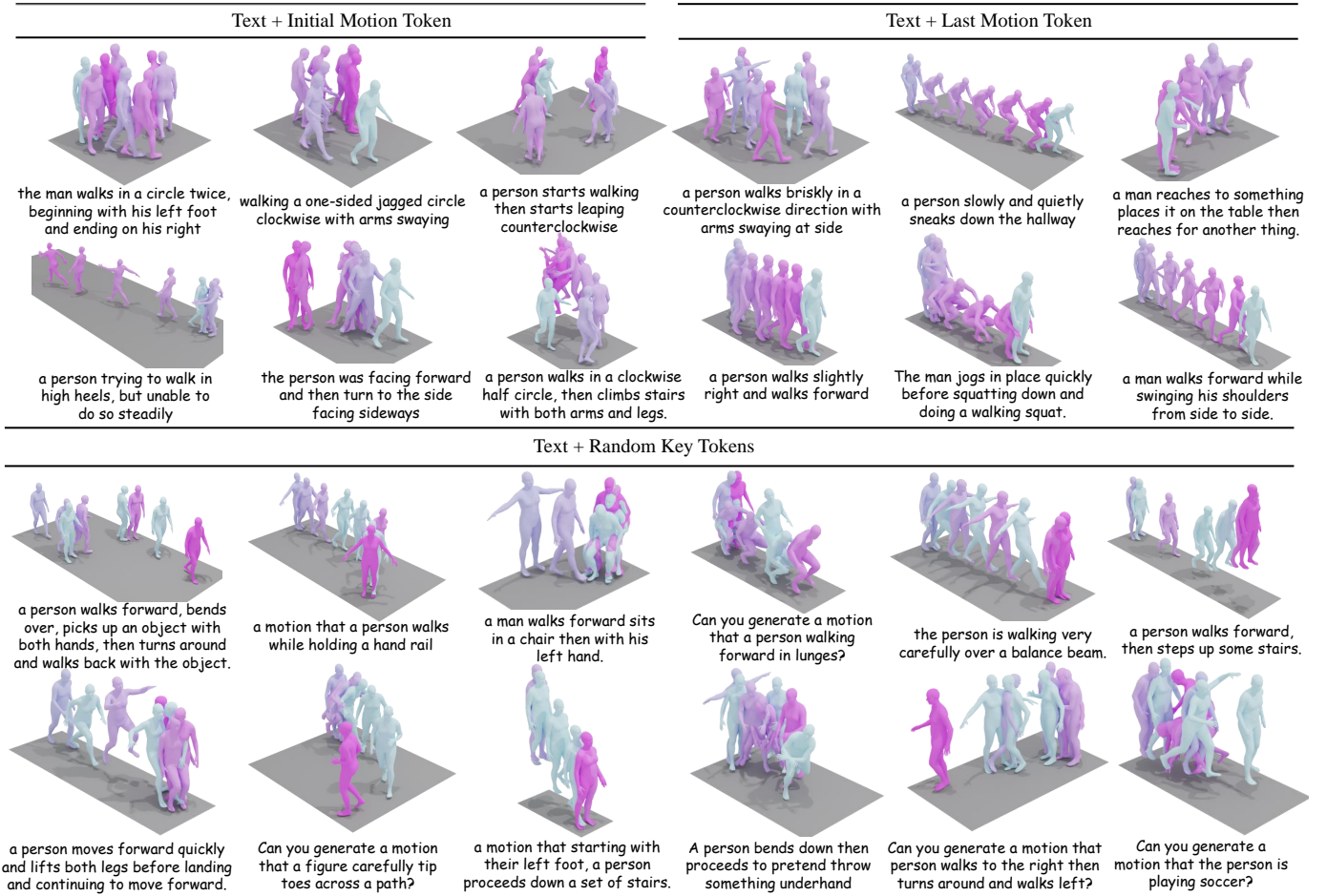


Fig. 9: Gallery showcasing the results of generated human motions by MotionGPT-2 with multiple control conditions on the HumanML3D dataset [20], i.e., *Text+Initial Motion Token*, *Text+Last Motion Token*, and *Text+Random Key Motion Token*. With these diverse control signals, our MotionGPT-2 demonstrates the ability to generate physically realistic human motions.

TABLE X: Evaluation of motion prediction and in-betweening on part of the AMASS [62] dataset, considering only motion data. FID reflects the quality of the generated motions, while Diversity quantifies the motion variability within each condition. ADE and FDE represent the distance between generated joint positions and the ground truth.

Methods	Motion Prediction				Motion In-between		
	FID ↓	Diversity↑	ADE↓	FDE↓	FID ↓	Diversity↑	ADE↓
Real	0.002	9.503	—	—	0.002	9.503	—
MDM [59]	6.031	7.813	5.446	8.561	2.698	8.420	3.787
MotionGPT [17]	0.905	8.972	4.745	6.040	0.214	9.560	3.762
MotionGPT-2 (Ours)	0.537	9.414	4.512	5.823	0.408	9.327	3.704

prompts. By constructing a unified motion-language vocabulary of LLM, we empower the pre-trained LLMs with the ability to integrate the understanding and generation of body kinetics. With well-designed Part-Aware VQVAE, MotionGPT-2 also demonstrates its versatility in addressing the complex 3D whole-body motion generation task, establishing a strong benchmark for researchers. We envision that MotionGPT-2 paves the way for more practical and versatile motion generation systems, offering a fresh perspective in the field.

B. Limitations

Our MotionGPT-2 primarily focuses on high-level semantic alignment between textual descriptions and motions. However, it captures finer semantic levels—such as the subtleties of body language, gestures, and contextual cues—less effectively. In the future, we will integrate visual data, e.g., videos, for physically realistic motion generation. Another limitation of our proposed MotionGPT-2 is its deficiency in interpreting and responding to dynamic environments or contextual interactions between humans and their surroundings. Future research aims to endow the MotionGPT-2 model with scene understanding and perception capabilities.

TABLE XI: Ablation study on the effects of the Part-Aware VQVAE (PA-VQVAE) on text-based motion generation, evaluated on Motion-X [28]. Along with full fine-tuning of the T5-base, LoRA-based fine-tuning [26] is used for optimizing other LLMs.

Model	Trainable Parameters	R-Precision \uparrow			FID \downarrow	MultiModal Dist. \downarrow	Diversity \rightarrow	MultiModality \uparrow
		Top 1	Top 2	Top 3				
Real	—	0.473	0.611	0.686	0.002	4.225	6.821	—
VQVAE (T5-base)	Full-Finetune	0.332	0.452	0.533	0.639	5.250	6.551	2.420
PA-VQVAE (T5-base)	Full-Finetune	0.349	0.473	0.544	0.628	5.164	6.596	2.322
VQVAE (Gemma-2B-It)	34M	0.334	0.467	0.552	0.639	5.038	6.848	2.311
PA-VQVAE (Gemma-2B-It)	34M	0.348	0.475	0.571	0.628	5.011	6.764	2.413
VQVAE (Gemma-7B-It)	101M	0.343	0.487	0.576	0.612	5.039	6.438	2.258
PA-VQVAE (Gemma-7B-It)	101M	0.377	0.507	0.583	0.620	4.819	6.267	2.146
VQVAE (LLaMA 3-8B)	89M	0.374	0.506	0.587	0.644	4.752	6.577	2.053
PA-VQVAE (LLaMA 3-8B)	89M	0.389	0.512	0.593	0.628	4.754	6.538	2.002
VQVAE (LLaMA 3.1-8B)	89M	0.387	0.521	0.601	0.666	4.673	6.446	2.352
PA-VQVAE (LLaMA 3.1-8B)	89M	0.398	0.522	0.616	0.619	4.656	6.574	2.821

TABLE XII: Performance evaluation of text-to-motion generation with **various LoRA parameters** on the HumanML3D test set using LLaMA 3-8B. The **best result** is highlighted in bold, and the second best result is underlined.

r	α	FID \downarrow	MultiModal Dist \downarrow	R-Precision \uparrow			Diversity \uparrow
				Top-1	Top-2	Top-3	
8	16	0.262	3.309	0.459	0.645	0.743	9.589
16	16	0.257	<u>3.168</u>	0.472	<u>0.658</u>	<u>0.755</u>	9.916
32	16	0.191	3.080	0.482	0.669	0.760	9.860
8	2	0.762	3.619	0.418	0.586	0.697	9.523
16	4	0.294	3.302	0.431	0.645	0.744	9.840
32	8	<u>0.217</u>	3.225	<u>0.477</u>	<u>0.658</u>	0.742	<u>9.885</u>
64	8	0.985	4.142	0.373	0.567	0.669	8.451
64	32	0.651	3.882	0.429	0.618	0.705	9.398
64	16	0.256	3.284	0.465	0.652	0.747	9.862

REFERENCES

- [1] Y. Zhang, D. Huang, B. Liu, S. Tang, Y. Lu, L. Chen, L. Bai, Q. Chu, N. Yu, and W. Ouyang, "Motiongpt: Finetuned llms are general-purpose motion generators," 2023.
- [2] C. Saharia, W. Chan, S. Saxena, L. Li, J. Whang, E. L. Denton, K. Ghasemipour, R. Gontijo Lopes, B. Karagol Ayan, T. Salimans et al., "Photorealistic text-to-image diffusion models with deep language understanding," *Advances in Neural Information Processing Systems*, vol. 35, pp. 36 479–36 494, 2022.
- [3] J. Yu, Y. Xu, J. Y. Koh, T. Luong, G. Baid, Z. Wang, V. Vasudevan, A. Ku, Y. Yang, B. K. Ayan et al., "Scaling autoregressive models for content-rich text-to-image generation," 2022.
- [4] A. Ramesh, P. Dhariwal, A. Nichol, C. Chu, and M. Chen, "Hierarchical text-conditional image generation with clip latents," 2022.
- [5] R. Rombach, A. Blattmann, D. Lorenz, P. Esser, and B. Ommer, "High-resolution image synthesis with latent diffusion models," in *Proceedings of the IEEE/CVF Conference on Computer Vision and Pattern Recognition*, 2022, pp. 10 684–10 695.
- [6] A. Ramesh, M. Pavlov, G. Goh, S. Gray, C. Voss, A. Radford, M. Chen, and I. Sutskever, "Zero-shot text-to-image generation," in *International Conference on Machine Learning*. PMLR, 2021, pp. 8821–8831.
- [7] L. Ouyang, J. Wu, X. Jiang, D. Almeida, C. Wainwright, P. Mishkin, C. Zhang, S. Agarwal, K. Slama, A. Ray et al., "Training language models to follow instructions with human feedback," *Advances in Neural Information Processing Systems*, vol. 35, pp. 27 730–27 744, 2022.
- [8] Z. Lu, D. Huang, L. Bai, X. Liu, J. Qu, and W. Ouyang, "Seeing is not always believing: A quantitative study on human perception of ai-generated images," 2023.
- [9] M. Petrovich, M. J. Black, and G. Varol, "Temos: Generating diverse human motions from textual descriptions," in *Computer Vision—ECCV 2022: 17th European Conference, Tel Aviv, Israel, October 23–27, 2022, Proceedings, Part XXII*. Springer, 2022, pp. 480–497.
- [10] M. Zhang, Z. Cai, L. Pan, F. Hong, X. Guo, L. Yang, and Z. Liu, "Motiondiffuse: Text-driven human motion generation with diffusion model," 2022.
- [11] G. Tevet, S. Raab, B. Gordon, Y. Shafir, D. Cohen-or, and A. H. Bermano, "Human motion diffusion model," in *The Eleventh International Conference on Learning Representations*, 2023. [Online]. Available: <https://openreview.net/forum?id=SJ1kSyO2jwu>
- [12] M. Petrovich, M. J. Black, and G. Varol, "Action-conditioned 3d human motion synthesis with transformer vae," in *Proceedings of the IEEE/CVF International Conference on Computer Vision*, 2021, pp. 10 985–10 995.
- [13] W. Zhuang, C. Wang, J. Chai, Y. Wang, M. Shao, and S. Xia, "Music2dance: Dancenet for music-driven dance generation," *ACM Transactions on Multimedia Computing, Communications, and Applications (TOMM)*, vol. 18, no. 2, pp. 1–21, 2022.
- [14] J. Zhang, Y. Zhang, X. Cun, S. Huang, Y. Zhang, H. Zhao, H. Lu, and X. Shen, "T2m-gpt: Generating human motion from textual descriptions with discrete representations," in *Proceedings of the IEEE/CVF Conference on Computer Vision and Pattern Recognition (CVPR)*, 2023.
- [15] X. Chen, B. Jiang, W. Liu, Z. Huang, B. Fu, T. Chen, and G. Yu, "Executing your commands via motion diffusion in latent space," in *Proceedings of the IEEE Conference on Computer Vision and Pattern Recognition*, 2023, pp. 18 000–18 010.
- [16] C. Guo, Y. Mu, M. G. Javed, S. Wang, and L. Cheng, "Momask: Generative masked modeling of 3d human motions," in *Proceedings of the IEEE Conference on Computer Vision and Pattern Recognition*, 2024, pp. 1900–1910.
- [17] B. Jiang, X. Chen, W. Liu, J. Yu, G. Yu, and T. Chen, "Motiongpt: Human motion as a foreign language," *Advances in Neural Information Processing Systems*, vol. 36, pp. 20 067–20 079, 2023.
- [18] M. Luo, R. Hou, H. Chang, Z. Liu, Y. Wang, and S. Shan, "M3gpt: An advanced multimodal, multitask framework for motion comprehension and generation," *arXiv preprint arXiv:2405.16273*, 2024.
- [19] M. Zhang, X. Guo, L. Pan, Z. Cai, F. Hong, H. Li, L. Yang, and Z. Liu, "Remodiffuse: Retrieval-augmented motion diffusion model," in *Proceedings of the IEEE/CVF International Conference on Computer Vision*, 2023, pp. 364–373.
- [20] C. Guo, S. Zou, X. Zuo, S. Wang, W. Ji, X. Li, and L. Cheng, "Generating diverse and natural 3d human motions from text," in *Proceedings of the IEEE/CVF Conference on Computer Vision and Pattern Recognition*,

- 2022, pp. 5152–5161.
- [21] D. Zhu, J. Chen, X. Shen, X. Li, and M. Elhoseiny, “Minigt-4: Enhancing vision-language understanding with advanced large language models,” 2023.
 - [22] Y. Du, K. Konyushkova, M. Denil, A. Raju, J. Landon, F. Hill, N. de Freitas, and S. Cabi, “Vision-language models as success detectors,” 2023.
 - [23] H. Liu, C. Li, Q. Wu, and Y. J. Lee, “Visual instruction tuning,” 2023.
 - [24] Q. Ye, H. Xu, G. Xu, J. Ye, M. Yan, Y. Zhou, J. Wang, A. Hu, P. Shi, Y. Shi, C. Jiang, C. Li, Y. Xu, H. Chen, J. Tian, Q. Qi, J. Zhang, and F. Huang, “implug-owl: Modularization empowers large language models with multimodality,” 2023.
 - [25] K. Li, Y. He, Y. Wang, Y. Li, W. Wang, P. Luo, Y. Wang, L. Wang, and Y. Qiao, “Videochat: Chat-centric video understanding,” 2023.
 - [26] E. J. Hu, Y. Shen, P. Wallis, Z. Allen-Zhu, Y. Li, S. Wang, L. Wang, and W. Chen, “Lora: Low-rank adaptation of large language models,” 2021.
 - [27] M. Plappert, C. Mandery, and T. Asfour, “The kit motion-language dataset,” *Big data*, vol. 4, no. 4, pp. 236–252, 2016.
 - [28] J. Lin, A. Zeng, S. Lu, Y. Cai, R. Zhang, H. Wang, and L. Zhang, “Motion-x: A large-scale 3d expressive whole-body human motion dataset,” *Advances in Neural Information Processing Systems*, vol. 36, 2024.
 - [29] J. Devlin, M.-W. Chang, K. Lee, and K. Toutanova, “Bert: Pre-training of deep bidirectional transformers for language understanding,” 2018.
 - [30] A. Radford, K. Narasimhan, T. Salimans, I. Sutskever et al., “Improving language understanding by generative pre-training,” 2018.
 - [31] A. Radford, J. Wu, R. Child, D. Luan, D. Amodei, and I. Sutskever, “Language models are unsupervised multitask learners,” 2019.
 - [32] T. Brown, B. Mann, N. Ryder, M. Subbiah, J. D. Kaplan, P. Dhariwal, A. Neelakantan, P. Shyam, G. Sastry, A. Askell et al., “Language models are few-shot learners,” *Advances in neural information processing systems*, vol. 33, pp. 1877–1901, 2020.
 - [33] OpenAI, “Gpt-4 technical report,” 2023.
 - [34] H. Touvron, T. Lavril, G. Izacard, X. Martinet, M.-A. Lachaux, T. Lacroix, B. Rozière, N. Goyal, E. Hambro, F. Azhar et al., “Llama: Open and efficient foundation language models,” 2023.
 - [35] C. Raffel, N. Shazeer, A. Roberts, K. Lee, S. Narang, M. Matena, Y. Zhou, W. Li, and P. J. Liu, “Exploring the limits of transfer learning with a unified text-to-text transformer,” *The Journal of Machine Learning Research*, vol. 21, no. 1, pp. 5485–5551, 2020.
 - [36] B. Lester, R. Al-Rfou, and N. Constant, “The power of scale for parameter-efficient prompt tuning,” 2021.
 - [37] X. Liu, K. Ji, Y. Fu, W. L. Tam, Z. Du, Z. Yang, and J. Tang, “P-tuning v2: Prompt tuning can be comparable to fine-tuning universally across scales and tasks,” 2021.
 - [38] S. Hu, N. Ding, H. Wang, Z. Liu, J. Wang, J. Li, W. Wu, and M. Sun, “Knowledgeable prompt-tuning: Incorporating knowledge into prompt verbalizer for text classification,” 2021.
 - [39] N. Houlsby, A. Giurgiu, S. Jastrzebski, B. Morrone, Q. De Laroussilhe, A. Gesmundo, M. Attariyan, and S. Gelly, “Parameter-efficient transfer learning for nlp,” in *International Conference on Machine Learning*. PMLR, 2019, pp. 2790–2799.
 - [40] R. He, L. Liu, H. Ye, Q. Tan, B. Ding, L. Cheng, J.-W. Low, L. Bing, and L. Si, “On the effectiveness of adapter-based tuning for pretrained language model adaptation,” 2021.
 - [41] H. Le, J. Pino, C. Wang, J. Gu, D. Schwab, and L. Besacier, “Lightweight adapter tuning for multilingual speech translation,” 2021.
 - [42] G. Tevet, B. Gordon, A. Hertz, A. H. Bermano, and D. Cohen-Or, “Motionclip: Exposing human motion generation to clip space,” in *Computer Vision–ECCV 2022: 17th European Conference, Tel Aviv, Israel, October 23–27, 2022, Proceedings, Part XXII*. Springer, 2022, pp. 358–374.
 - [43] I. Habibie, D. Holden, J. Schwarz, J. Yearsley, and T. Komura, “A recurrent variational autoencoder for human motion synthesis,” in *Proceedings of the British Machine Vision Conference (BMVC)*, 2017.
 - [44] Z. Li, Y. Zhou, S. Xiao, C. He, Z. Huang, and H. Li, “Auto-conditioned recurrent networks for extended complex human motion synthesis,” 2017.
 - [45] C. Guo, X. Zuo, S. Wang, S. Zou, Q. Sun, A. Deng, M. Gong, and L. Cheng, “Action2motion: Conditioned generation of 3d human motions,” in *Proceedings of the 28th ACM International Conference on Multimedia*, 2020, pp. 2021–2029.
 - [46] R. Li, S. Yang, D. A. Ross, and A. Kanazawa, “Ai choreographer: Music conditioned 3d dance generation with aist++,” in *Proceedings of the IEEE/CVF International Conference on Computer Vision*, 2021, pp. 13401–13412.
 - [47] E. Barsoum, J. Kender, and Z. Liu, “Hp-gan: Probabilistic 3d human motion prediction via gan,” in *Proceedings of the IEEE conference on computer vision and pattern recognition workshops*, 2018, pp. 1418–1427.
 - [48] J. Martinez, M. J. Black, and J. Romero, “On human motion prediction using recurrent neural networks,” in *Proceedings of the IEEE conference on computer vision and pattern recognition*, 2017, pp. 2891–2900.
 - [49] K. Kania, M. Kowalski, and T. Trzciński, “Trajevae: Controllable human motion generation from trajectories,” 2021.
 - [50] A. Ghosh, N. Cheema, C. Oguz, C. Theobalt, and P. Slusallek, “Synthesis of compositional animations from textual descriptions,” in *Proceedings of the IEEE/CVF International Conference on Computer Vision*, 2021, pp. 1396–1406.
 - [51] C. Ahuja and L.-P. Morency, “Language2pose: Natural language grounded pose forecasting,” in *2019 International Conference on 3D Vision (3DV)*. IEEE, 2019, pp. 719–728.
 - [52] C. Guo, X. Zuo, S. Wang, and L. Cheng, “Tm2t: Stochastic and tokenized modeling for the reciprocal generation of 3d human motions and texts,” in *Computer Vision–ECCV 2022: 17th European Conference, Tel Aviv, Israel, October 23–27, 2022, Proceedings, Part XXXV*. Springer, 2022, pp. 580–597.
 - [53] A. Radford, J. W. Kim, C. Hallacy, A. Ramesh, G. Goh, S. Agarwal, G. Sastry, A. Askell, P. Mishkin, J. Clark et al., “Learning transferable visual models from natural language supervision,” in *International conference on machine learning*. PMLR, 2021, pp. 8748–8763.
 - [54] Q. Wu, Y. Zhao, Y. Wang, Y.-W. Tai, and C.-K. Tang, “Motionllm: Multimodal motion-language learning with large language models,” *arXiv preprint arXiv:2405.17013*, 2024.
 - [55] A. Van Den Oord, O. Vinyals et al., “Neural discrete representation learning,” *Advances in neural information processing systems*, vol. 30, 2017.
 - [56] S. Lu, L.-H. Chen, A. Zeng, J. Lin, R. Zhang, L. Zhang, and H.-Y. Shum, “Humantomato: Text-aligned whole-body motion generation,” *arXiv preprint arXiv:2310.12978*, 2023.
 - [57] M. Zhang, Z. Cai, L. Pan, F. Hong, X. Guo, L. Yang, and Z. Liu, “Motiondiffuse: Text-driven human motion generation with diffusion model,” *IEEE Transactions on Pattern Analysis and Machine Intelligence*, 2024.
 - [58] J. Wei, M. Bosma, V. Y. Zhao, K. Guu, A. W. Yu, B. Lester, N. Du, A. M. Dai, and Q. V. Le, “Finetuned language models are zero-shot learners,” 2021.
 - [59] G. Tevet, S. Raab, B. Gordon, Y. Shafir, D. Cohen-Or, and A. H. Bermano, “Human motion diffusion model,” in *The Eleventh International Conference on Learning Representations*, 2023. [Online]. Available: <https://openreview.net/forum?id=SJ1kSyO2jwu>
 - [60] C. Zhong, L. Hu, Z. Zhang, and S. Xia, “Att2m: Text-driven human motion generation with multi-perspective attention mechanism,” in *Proceedings of the IEEE/CVF International Conference on Computer Vision*, 2023, pp. 509–519.
 - [61] P. Jin, Y. Wu, Y. Fan, Z. Sun, W. Yang, and L. Yuan, “Act as you wish: Fine-grained control of motion diffusion model with hierarchical semantic graphs,” *Advances in Neural Information Processing Systems*, vol. 36, 2024.
 - [62] N. Mahmood, N. Ghorbani, N. F. Troje, G. Pons-Moll, and M. J. Black, “Amass: Archive of motion capture as surface shapes,” in *Proceedings of the IEEE/CVF international conference on computer vision*, 2019, pp. 5442–5451.
 - [63] C. Mandery, Ö. Terlemez, M. Do, N. Vahrenkamp, and T. Asfour, “The kit whole-body human motion database,” in *2015 International Conference on Advanced Robotics (ICAR)*. IEEE, 2015, pp. 329–336.
 - [64] C. G. Lab, “Cmu graphics lab motion capture database,” <http://mocap.cs.cmu.edu/>, 2000.
 - [65] G. Pavlakos, V. Choutas, N. Ghorbani, T. Bolkart, A. A. Osman, D. Tzionas, and M. J. Black, “Expressive body capture: 3d hands, face, and body from a single image,” in *Proceedings of the IEEE/CVF conference on computer vision and pattern recognition*, 2019, pp. 10975–10985.
 - [66] K. Papineni, S. Roukos, T. Ward, and W.-J. Zhu, “Bleu: a method for automatic evaluation of machine translation,” in *Proceedings of the 40th annual meeting of the Association for Computational Linguistics*, 2002, pp. 311–318.
 - [67] C.-Y. Lin, “Rouge: A package for automatic evaluation of summaries,” in *Text summarization branches out*, 2004, pp. 74–81.
 - [68] R. Vedantam, C. Lawrence Zitnick, and D. Parikh, “Cider: Consensus-based image description evaluation,” in *Proceedings of the IEEE conference on computer vision and pattern recognition*, 2015, pp. 4566–4575.
 - [69] T. Zhang, V. Kishore, F. Wu, K. Q. Weinberger, and Y. Artzi, “Bertscore: Evaluating text generation with bert,” *arXiv preprint arXiv:1904.09675*, 2019.

- [70] H. Ma, J. Li, R. Hosseini, M. Tomizuka, and C. Choi, “Multi-objective diverse human motion prediction with knowledge distillation,” in Proceedings of the IEEE Conference on Computer Vision and Pattern Recognition, 2022, pp. 8161–8171.
- [71] Y. Yuan and K. Kitani, “Dlow: Diversifying latent flows for diverse human motion prediction,” in Computer Vision–ECCV 2020: 16th European Conference, Glasgow, UK, August 23–28, 2020, Proceedings, Part IX 16. Springer, 2020, pp. 346–364.
- [72] I. Loshchilov and F. Hutter, “Decoupled weight decay regularization,” 2017.
- [73] Y. Zhang, M. J. Black, and S. Tang, “We are more than our joints: Predicting how 3d bodies move,” in Proceedings of the IEEE Conference on Computer Vision and Pattern Recognition, 2021, pp. 3372–3382.